Marine and Petroleum Geology 145 (2022) 105871

Contents lists available at ScienceDirect

Marine and Petroleum Geology

journal homepage: www.elsevier.com/locate/marpetgeo

Interaction of inherited structures and contractional deformation in the South Dezful Embayment: Insights from the Gachsaran oilfield, SW Iran

Aref Shamszadeh [a,*], Khalil Sarkarinejad [a], Oriol Ferrer [b], Soumyajit Mukherjee [c], Mohammad Seraj [d]

[a] Department of Earth Sciences, College of Sciences, Shiraz University, Shiraz, Iran
[b] Institut de Recerca Geomodels, Universitat de Barcelona, Martí i Franquès s/n, 08028, Barcelona, Spain
[c] Department of Earth Sciences, Indian Institute of Technology Bombay, Powai, Mumbai, 400 076, Maharashtra, India
[d] National Iranian South Oil Company (NISOC), Ahwaz, Iran

ARTICLE INFO

Keywords:
Dezful Embayment
Zagros
Structural inheritance
Kharg-Mish

ABSTRACT

Identifying the timing, geometry, mechanism and multiphase reactivation of the inherited structures on the structural style of the fold-and-thrust belt is important for hydrocarbon exploration and production.

In this work, we present a multidisciplinary approach including field data, seismic profiles, well data analyses, isopach maps, 2D balanced cross-sections construction, and 2D sequential restoration. Such an approach is applied to decipher the multiphase deformation of the NNE-SSW trending deep-seated Kharg-Mish Fault (KMF) that controlled the tectono-sedimentary evolution and structural style of the Gachsaran Anticline (South Dezful Embayment - SDE). Kinematic analysis of the KMF reveals two different mechanisms from normal to reverse faulting (positive inversion) since the Cenomanian. From the Late Cretaceous-Late Miocene, the sedimentary cover thickness ~2500 m decreases along-strike of the Gachsaran Anticline towards the east, over the KMF, due to regional erosion and pinch-out.

The eastern sector of the Gachsaran Anticline shows an angular and smaller wavelength fold in the levels of Asmari and Sarvak formations due to the efficient local middle décollements of the Kazhdumi and Pabdeh formations. Different amounts of shortening, 19.4% for the western and 16.7% for the eastern sector, and fore-thrust propagation developed a tear fault that accommodated differential deformation. Long-term structural evolution and strain localization in the eastern sector of the Gachsaran Anticline over the KMF produced dense fracturing. Our study suggests that mechanism and timing of deformation along the pre-existing basement structures are important in structural evolution of the sedimentary cover, oil migration and accumulation in such a hydrocarbon province.

1. Introduction

Tectonic inheritance is of global attention to academia and oil industry (e.g. Butler et al., 2006; Cooper et al., 1989; Misra and Mukherjee, 2015). Understanding the relationship between pre-existing basement fault reactivation, lateral thickness and facies variation of sedimentary cover, and contractional deformation of the Zagros fold-and-thrust belt (ZFTB) are critical to decipher different structural styles of the South Dezful Embayment (SDE). In terms of hydrocarbon production and exploration, these factors are important for an accurate evaluation of the fold style, timing and petroleum basin prospectivity (e.g. Bordenave and Hegre, 2005; Riahi et al., 2021).

The sedimentary infill of the SDE is affected by two NNE-SSW trending basement-involved faulted highs, Hendijan-Bahregansar-Nowrooz and Kharg-Mish, that control facies changes and overburden thickness variations during the Phanerozoic (Abdullahie Fard et al., 2006; Bahroudi and Koyi, 2003; Farahzadi et al., 2019; Motiei, 1994; Noori et al., 2019; Riahi et al., 2021; Shamszadeh et al., 2022; Sherkati and Letouzey, 2004). Several studies have addressed the effect of lateral and vertical variation of the sedimentary cover on the fold style and geometry in fold-and-thrust belts (Table 1; Nabavi and Fossen, 2021; Ramsay, 1967). In addition, the role of the pre-existing basement faults as weakness places in controlling the structural evolution and fold style of the overburden is critical during the contractional deformation

* Corresponding author.
E-mail address: arefshams70@gmail.com (A. Shamszadeh).

https://doi.org/10.1016/j.marpetgeo.2022.105871
Received 12 February 2022; Received in revised form 12 July 2022; Accepted 6 August 2022
Available online 14 August 2022

Table 1
A summary of several works that evaluated the effective parameters on fold style and geometry in fold-and-thrust belts.

Author	Approach	Key finding	Natural example/ General concept (GC)
Currie et al. (1962)	Field observation, Experimental modeling	The physical properties and thickness of a dominant member control the fold wavelength that develops in the early stages of deformation	GC
Sherkati et al. (2006)	Analog modeling, cross-section, seismic data	Thickness and mechanical rheology of sedimentary cover affect the style and wavelength of folds	Central Zagros fold and thrust belt, Iran
Sepehr et al. (2006)	Cross-section, Field observation	The thickness and facies distribution of the cover rock succession has a significant impact on the style of deformation	Zagros fold-and-thrust belt, Iran
Motamedi et al. (2012)	Seismic interpretation, cross-section	Variation in structural style is related to variations in the thickness and distributions of the major tectonostratigraphic units	Central Fars area, Zagros fold-and-thrust belt
Butler et al. (2018)	Seismic interpretation, Cross-section	Changes in structural style are related to pre-kinematic stratigraphic variations	GC
Meng and Hodgetts (2019)	Numerical experiments	Cover rock cohesion and décollement layer thickness affect the surface uplift, fold amplitude, and propagation rate of deformation	GC

Table 2
A summary of several works that evaluated the effect of pre-existing structures in controlling structural deformation.

Author	Approach	Key finding	Natural example/ General concept (GC)
Giambiagi et al. (2003)	Cross-section	Shortening was accommodated by a combination of inversion of pre-existing normal faults	Aconcagua fold and thrust belt, southern Andes
Scisciani (2009)	Cross-section, field studies	The pre-existing normal faults constituted important mechanical anisotropies that were effective in controlling the localization, spacing, and kinematics of the propagating thrust ramps and related fold nucleation within the sedimentary cover	Central Apennines and the Adriatic foreland
Tong et al. (2014)	Analog modeling	The formation and propagation of faults can be triggered very early by pre-existing rigid-border faults	GC
Koyi et al. (2016)	Analog modeling	The importance of basement reactivation timing with respect to the shortening	GC/Alborz mountains and Zagros fold and thrust belt, Iran
Burberry and Swiatlowski (2016)	Analog modeling	Pre-existing structure promotes the development and clustering of branch lines in the overlying thrust faults	GC
Schori et al. (2021)	Analog modeling	Upward and downward pre-existing steps localizing deformation.	Jura Mountains Fold-and-Thrust Belt

(Table 2).

The Dezful Embayment in the Zagros foreland folded belt has been recognized as one of the greatest oil provinces globally due to the discovery of several oilfields (e.g., the Gachsaran, Parsi, and Rag-e-Sefid among others). However, the regional structural framework of these fields is not well understood especially in the context of the pre-existing basement faults. In this article, we study the Gachsaran oilfield, a subsurface structure in the north of the SDE. The impact of the Kharg-Mish Fault (KMF) on the eastern sector of the Gachsaran Anticline gives structural complexities in terms of fold style and structural evolution of the studied anticline in comparison to the western sector.

This study aims to determine the structural evolution and fold style of the Gachsaran Anticline, by 2D seismic sections, well data, and isopach maps. To fully understand the fold style and geometry of the structure, pre-shortening basin configuration, and inherited structures are to be understood. For this purpose, 2D sequential restorations along strike of the Gachsaran fold axis and perpendicular to the KMF have been constructed to understand the detailed tectonic-sedimentary evolution and multi-episodic deformation. Further, we have mainly focused on the structural evolution of the eastern part of the Gachsaran Anticline where the deep-rooted structure related to the KMF reactivation was overprinted by the ZFTB shortening since Early Cretaceous up to the recent.

2. Tectonics & stratigraphy

The Zagros fold-and-thrust belt (ZFTB), a part of the Late Cretaceous to Tertiary Alpine- Himalayan orogenic belt, resulted from the Neo-Tethyan Ocean closure between the north of the Gondwana and south of the Laurasia margins. The NW-SE trending ZFTB with ~2000 km long (Alavi, 1994, 2007; Berberian and King, 1981; Mouthereau et al., 2012; Vergés et al., 2011) introduces a 25° oblique transpression zone between the Afro-Arabian plate in the SW and the Iranian micro-plate in the NE (Sarkarinejad and Azizi, 2008). The inherited N-S to NW-SE trending basement faults in the NE margin of the Arabian plate from Pan-African orogeny (670-570 Ma), divide the ZFTB into different tectonostratigraphic zones (e.g. Alavi, 2007; Falcon, 1974; Mouthereau et al., 2012; Sarkarinejad and Goftari, 2019). The Zagros orogen is divided into six main sub-parallel distinct belts (Vergés et al., 2011; Sarkarinejad and Goftari, 2019). From NE to SW these are (1) the Uromieh-Dokhtar volcanic arc (UDVA), (2) the Sanandaj- Sirjan metamorphic belt, (3) Imbricated Zone, (4) the Zagros Foreland fold-and-thrust belt (High Zagros Belt), (5) the Zagros foreland folded belt, and (6) the Mesopotamian-Persian Gulf Foreland basin (Fig. 1). In the central part of the Zagros foreland folded belt, the Mountain Front Flexure, a fault zone rooted from the NW-SE basement step, separates the Izeh Zone in the NE from the Dezful Embayment in the SW. The Dezful Embayment is bounded by two transverse basement faults: the Kazerun Fault at the SE and the Bala Rud Fault at the NW (Fig. 1; e.g. Berberian, 1995; Mouthereau et al., 2012).

Different tectonic events since the Late Proterozoic affected the sedimentary basin of the Dezful Embayment (e.g. Motiei, 1995; Sherkati and Letouzey, 2004). One of the important events is related to the transtensional phase that produced the Najd system, during the Late Proterozoic (Al-Husseini, 2000; Bahroudi and Talbot, 2003; Husseini, 1989; Talbot and Alavi, 1996). Different shallow pull-apart basins mainly along strike the N-S basement faults have controlled the epicontinental deposition of the Neoproterozoic-Cambrian Hormuz series at this time (Edgell, 1996; Faqira et al., 2009; Mukherjee et al., 2010; Mukherjee, 2011; Perotti et al., 2011; Stewart, 2018). Several studies on the fold style and geometry of the Dezful Embayment structures have considered a main basal décollement (probably the Hormuz series) during the evolution of the structures (e.g. Carruba et al., 2006; Colman-Sadd, 1978; Derikvand et al., 2018; Heydarzadeh et al., 2020).

Shallow marine platform shales and sandstones developed in the Hormuz basin until the Carboniferous time (e.g. Stampfli and Borel,

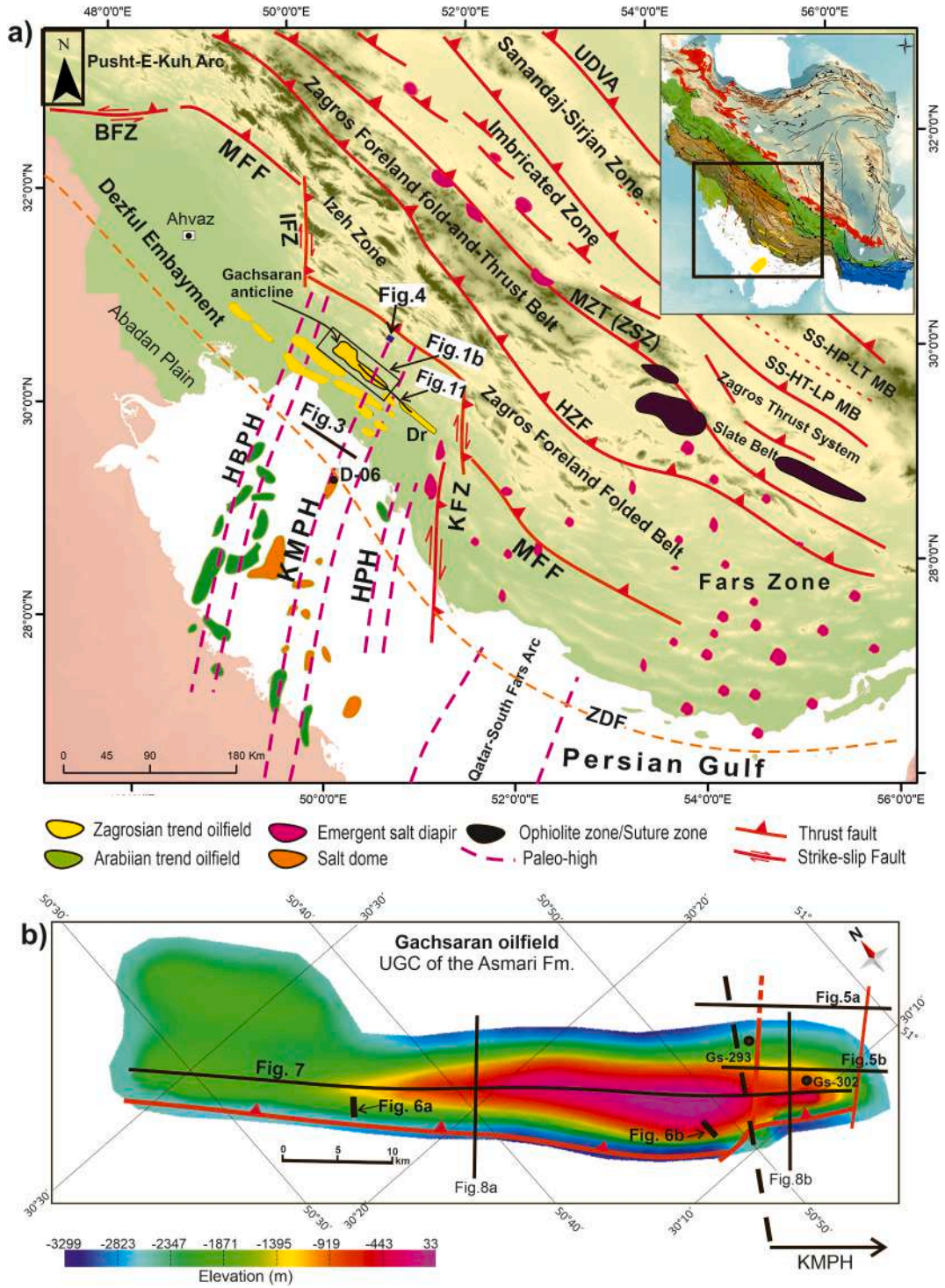

Fig. 1. a) Geological map with the main structural elements of the Zagros fold-and-thrust belt (modified after Berberian, 1995; Derikvand et al., 2018; Edgell, 1996; Jahani et al., 2017; Perotti et al., 2011; Sarkarinejad and Goftari, 2019; Stewart et al., 2018; Soleimany et al., 2011; Tavakoli-Shirazi et al., 2013). Inset map: location of the region on the geological map of Iran. (b) The depth map at the top Asmari Formation of the Gachsaran Anticline (black rectangle in Fig. 1a). BFZ; Bala Rud Fault Zone; D: Dorood oilfield; Dr: Dara anticline; Gs: Gachsaran oilfield; HBPH: Hendijan-Bahregansar Paleo High; HZF: High Zagros Fault; IFZ: Izeh Fault Zone; KMPH: Kharg-Mish Paleo-High; KZF; Kazerun Fault Zone; MFF; Mountain Front Flexure; MZT: Main Zagros Thrust; SS HP-LT MB: Sanandaj-Sirjan HP-LT Metamorphic Belt; SS HT-LP MB: Sanandaj-Sirjan HT-LP Metamorphic Belt; UDVA: Uromieh-Dokhtar Volcanic Arc; ZDF: Zagros Deformation Thrust; ZSZ: Zagros Suture Zone.

2002; Perotti et al., 2011). Besides sparse outcrops in the High Zagros, characteristics of Paleozoic rocks in the study area are unknown due to the lack of outcrops and well data. Due to huge erosion related to the Hercynian orogeny (e.g., Asl et al., 2019;Faqira et al., 2009), one of the important events in the NE of Gondwana in the Carboniferous, it is difficult to constrain the Cambrian-Carboniferous thicknesses and tectonostratigraphy (e.g. Konert et al., 1999; Stewart, 2018). Red conglomerates and sandstones at the base of the Faraghan Formation indicate Permo-Triassic transgression (Alavi, 2007).

During the Permo-Triassic, the opening of the Neo-Tethyan oceanic

crust separated the Afro-Arabian and micro-Iranian plates towards the SW and NE, respectively. During this Permo-Triassic period, shallow-marine carbonates of the Dalan and Kangan formations (Dehram Group), one of the main gas reservoirs in the ZFTB, deposited in the NE passive margin of the Afro-Arabian plate (Alavi, 2004; Sepehr and Cosgrove, 2004). Across the NW-SE trending of extensional passive margin faults in the NE of the Arabian plate, which also acts as facies boundary, Khanehkat carbonate formation changes to Dashtak evaporites from the Izeh Zone in the NE towards the Dezful Embayment in the SW (e.g.; Sepehr and Cosgrove, 2004; Szabo and Kheradpir, 1978). Triassic Dashtak evaporites are the main intermediate decollement in most of the structures of the ZFTB (e.g., Abdullahie Fard et al., 2006;

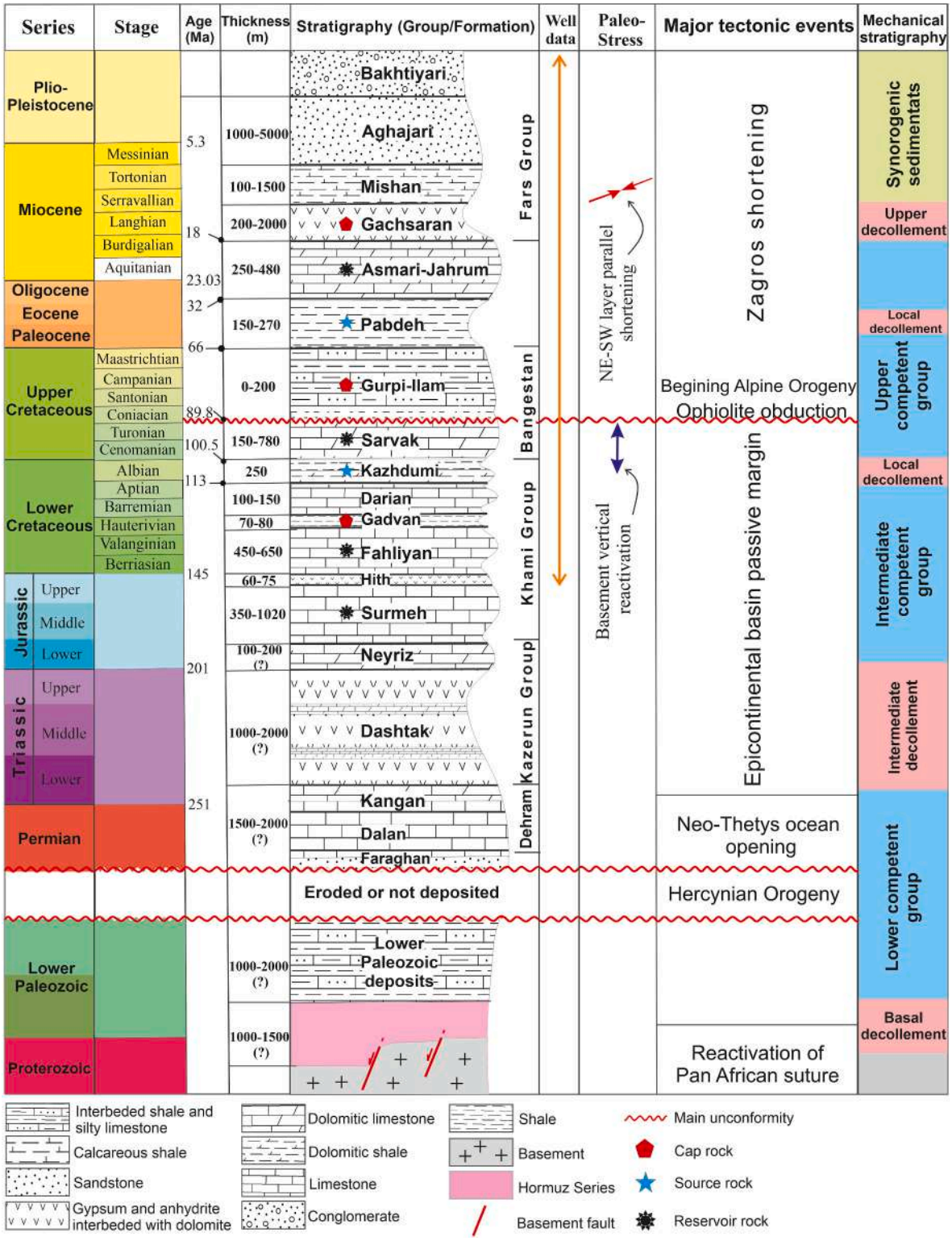

Fig. 2. Tectonostratigraphiy of the South Dezful Embayment based on surface and subsurface data. The thickness and mechanical stratigraphy down to the Surmeh Formation is based on this study and is completed based on, Abdullahie Fard et al. (2006), Alavi (2004), Derikvand et al. (2018), Sherkati and Letouzey (2004), and Soleimany et al. (2011).

Najafi et al., 2014).

The Jurassic-Lower Cretaceous sedimentary thickness and facies of the Khami Group vary laterally (between the carbonate to shale and evaporites formations) across the Kazerun, Bala Rud, and Izeh Fault Zone towards the Dezful Embayment (Setudehnia, 1978; Sepehr and Cosgrove, 2004). This Middle-Upper Jurassic-Lower Cretaceous Group including the Surmeh, Hith, Fahliyan, Gadvan, and Dariyan formations have been drilled by several wells in the study area (down to the ~ −3600 m). This Jurassic-Lower Cretaceous mega-sequence unconformably overlies the Permo-Triassic sequences as the Neo-Tethyan ocean rifted in the Mid to Late Permian (Alavi, 2007; Berberian and King, 1981; Koop and Stoneley, 1982). It is also unconformably overlain by the Albian shales of the Kazhdumi Formation (~250 m), which is one of the source rocks in the Dezful Embayment.

From the Cenomanian up to Campanian, another mega-sequence of carbonates includes the Sarvak and Ilam formations deposited in a shallow continental shelf basin in the ZFTB (Alavi, 2004). Another main disconformity clearly apparent resulted in response to the first stage of Alpine orogeny with the onset of ophiolitic obduction during the Turonian (e.g. Abdullahie Fard et al., 2006; Farahzadi et al., 2019; Moghadam et al., 2013). Upper Cretaceous sediments were either significantly eroded or not deposited, up to 80%, in the study area. The Turonian unconformity contact is overlain by shallow marine carbonates to continental siliciclastic deposits of the Late Cretaceous derived from the Zagros hinterland part (Alavi, 2004). Marine shales, marls, and marly limestones of the Late Cretaceous-Eocene Pabdeh and Gurpi formations are the source rocks. They supply oil to the overlaying 250–450 m thick Oligocene-Early Miocene shallow marine limestones of the Asmari Formation, the main reservoir in the Dezful Embayment (Carruba et al., 2006).

Very thick (>5000 m) Mio-Pleistocene post-collision sequence including Gachsaran, Mishan, Aghajari and Bakhtiyari formations (Fars Group) deposited in the Dezful Embayment (Pirouz et al., 2017). The Gachsaran evaporites as caprock of the Asmari reservoir formed a major upper décollement in the Dezful Embayment (e.g., Bahroudi and Koyi, 2003; Derikvand et al., 2018). Overall, the total thickness of the sedimentary sequences over the heterogeneous basement ranges from ~7 to 12 km in the Dezful Embayment (Fig. 2; e.g. Alavi, 2004, 2007; Carruba et al., 2006; Sherkati and Letouzey, 2004).

3. Dataset &methods

Seismic and well data, field observations, and balanced cross-sections have been used in this work. 2D seismic and well data were provided by the National Iranian South Oil Company (NISOC). More than 400 wells drilled in the Gachsaran oilfield (down to the Hith Formation ~ −3600 m depth) have been used to constrain the six isopach maps presented in this work. 2D sequential restoration, isopach maps, balanced cross-sections, and well correlation profiles were used to elucidate the tectonic-sedimentary evolution of the study area. During the sequential restoration, ten interpreted horizons from the top Gadvan Formation to recent deposits, were back-stripped sequentially by unfaulting, unfolding, and decompaction. Midland Valley Move software (2018) has been used for the 2D sequential restoration of a section along strike and for construction of two balanced cross-sections across the Gachsaran Anticline. For the decompaction process, the mechanical properties of the rock units were calculated by the geomechanical evaluation of several drilled wells of the Gachsaran oilfield in the Geomechanics Department of the NISOC (Table 3). The average values of the mechanical parameters (Young's modulus, Poisson's ratio, Bulk density, porosity, and friction angle) have been used for some formations with multiple lithologies. Athy's law (Dasgupta and Mukherjee, 2020) was followed for the porosity/depth relation (Eq. (1)):

$$f = f_0 (\exp)^{(-cz)} \quad (1)$$

Table 3
Mechanical properties and decompaction parameters of each formation were used in the restoration techniques of this study.

Formation	Static Young's modulus (MPa)	Poisson's Ratio (Unitless)	Bulk Density (kg m^{-3})	Porosity (Unitless)	Friction Angle (Degree)
Aghajari	27,140	0.33	2650	12	30
Mishan	7250	0.36–0.4	2450	15–20	20
Gachsaran	10,350	0.4	2530	14	26
Asmari	36,400	0.29	2650	6–10%	35
Jahrum	31,200	0.31	2620	8–10%	25
Pabdeh	23,450	0.35	2580	12	20
Gurpi	35,400	0.28	2680	2–5%	34
Ilam-Sarvak	35,500	0.33	2580	15–20	26
Kazhdumi	36,100	0.32	2610	3–10%	28
Dariyan	27,700	0.33	2430	13	25
Gadvan	27,200	0.33	2610	12	30

Here f: porosity at depth z, f_0: surface porosity, c: porosity/depth coefficient.

For the standard value of the f_0 and c, we utilized the default compaction curve for the area with mixed lithology provided in Move software, which is based on Sclater and Christie (1980). Furthermore, for the 2D backstriping of the section, the paleobathymetry values for each formation have been provided by the biostratigraphic data in some wells of the Gachsaran oilfield.

4. Structural analyses

4.1. Impact of the Kharg-Mish Fault on the sedimentary cover

Reactivation of ~ N-S trending of the Kharg-Mish Fault (KMF) as a pre-existing basement extensional fault has affected the basin-fill of the SDE (Ahmadhadi et al., 2007; Mouthereau et al., 2007; Sherkati and Letouzey, 2004; Soleimany et al., 2011). Structural features of the KMF were detected through detailed geologic analyses of the surface and subsurface data. A linear arrangement of the offshore oilfields (Fig. 1), the curvature of the fold axis traceable in the onshore structures, and subsurface evidence such as thickness and facies variation of the sedimentary cover related to the reactivation of this fault during the Phanerozoic suggest that the fault extends from the southern part of the Persian Gulf to the north of the SDE (e.g. Shamszadeh et al., 2022; Motiei, 1994).

The seismic profile across the KMF reveals that severe structural amplification happened along the fault began from the Cenomanian and reached a peak at Turonian time (Fig. 3). This is documented by a huge erosion or/non deposition of the Bangestan Group. A large thinning (from ~950 m to ~ 100 m) of the Upper Cretaceous Bangestan Group (Ilam-Sarvak formations) atop of the deep-seated buried anticline can be observed across the KMF (Fig. 3).

The interpreted top-formation horizons on the seismic section at least reveal the thickness variation patterns of the strata down to the Uppermost Jurassic Hith Formation. The Bangestan Group and the Plio-Pleistocene Upper Aghajari-Bakhtiyari formations on both sides of the salt-cored structure show considerable growth thinning strata towards the crest of the structure (Fig. 3). Deep-seated fault reactivation of the KMF has probably controlled this circular to elongated salt-related structure (e.g. Sherkati and Letouzey, 2004; Soleimany et al., 2011). The geometry of the interpreted top-formtions demonstrates the deformation along the KMF initiated at least from the Late Cretaceous, which thinned of the layers from the flanks towards the structure (Fig. 3). Therefore, the buried salt-related anticline (e.g. Shamszadeh et al., 2022; Soleimany et al., 2011) along the KMF is considered as a growth structure developed by multiple reactivations of the KMF during the Late Cretaceous-Recent time (Fig. 3).

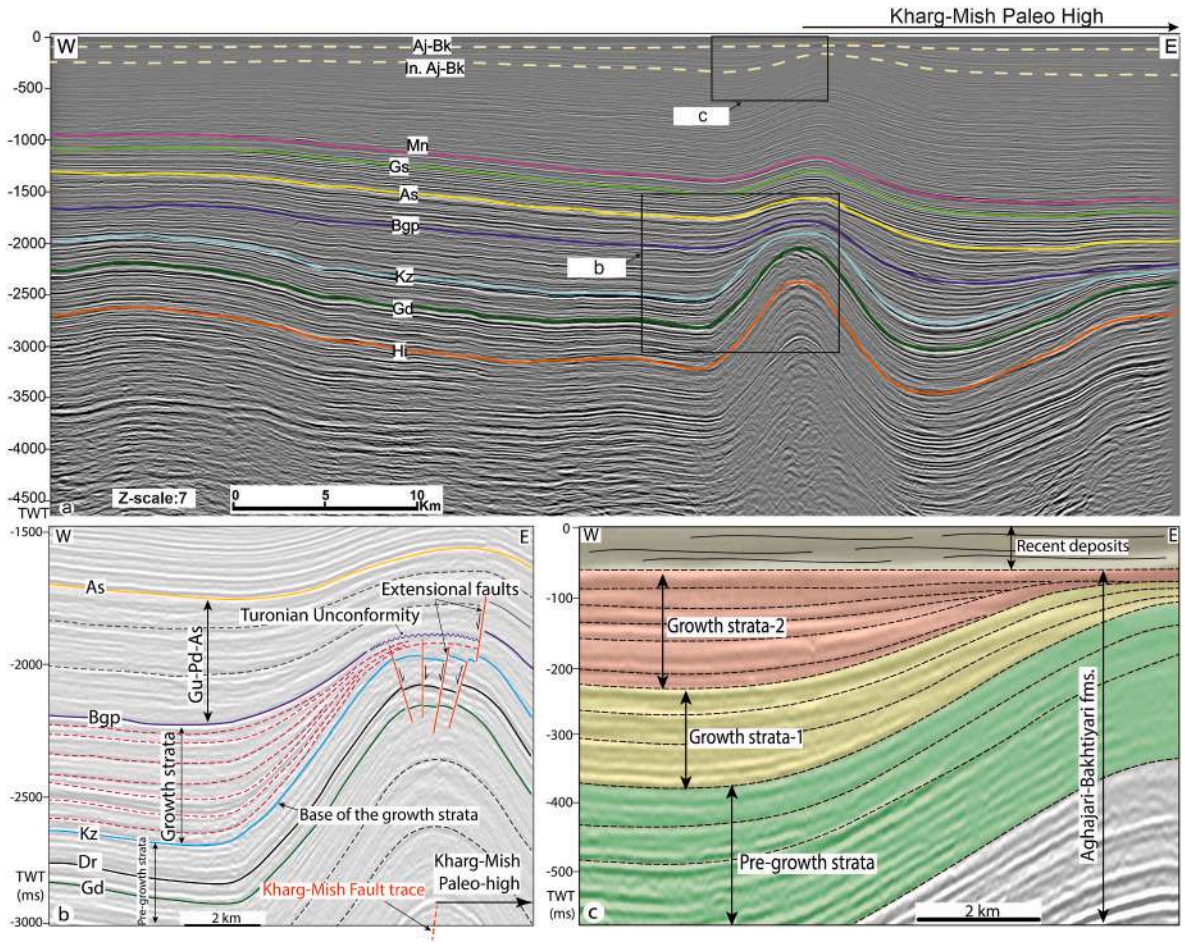

Fig. 3. a) An interpreted 2D seismic profile across the Kharg-Mish and Hendijan-Bahregansar Paleo highs. See Fig. 1 for location. b) and c) close-up pictures of the Late Cretaceous Bangestan Group and Plio-Pleistocene Upper Aghajari-Bakhtiyari growth strata, respectively. See Fig. 3a for location. As: Top Asmari Formation; Bgp: Top Bangestan group; Gd: Top Gadvan Formation; Hi: Top Hith Formation; In. Aj-Bk: Intra Aghajari-Bakhtiyari formations; Gs: Top Gachsaran Formation; KMPH: Kharg-Mish Paleo-High; KMZ: Kharg-Mish Paleo High; Kz: Top Kazhdumi Formation; Mn: Top Mishan Formation; TWT: Two Way Time. Uninterpreted sections have been provided in Repository data No.1.

The Kharg-Mish Fault continued to the Mish anticline in the Izeh Zone, north of the Gachsaran Anticline. Field observation data indicates the depositional geometry of the Oligo-Miocene Asmari Formation in the Mish anticline was affected by the reactivation/or trace of the KMF (Fig. 4). The platform of the Asmari Formation developed around the shelf-margin delta prograding into pre-existing highstand area created by the KMF. Fig. 4 shows a large-scale NNE prograding clinoform geometry of the Asmari Formation in the SW flank of the Mish anticline. This stratal pattern clearly demonstrates the interplay amongst sediment supply, tectonics and sea-level changes.

4.2. Effect of the KMF at the eastern sector of the Gachsaran Anticline

W-E seismic sections along the eastern sector of the Gachsaran Anticline displays the gradual thinning of the Upper Cretaceous Bangestan Group towards the east (Fig. 5a). Also, the seismic profile at the north of the Gachsaran Anticline clearly shows a normal displacement over a high-angle fault (Fig. 5a). However, this dip-slip fault has not been well interpreted in the section above the Gachsaran Anticlinal crest (Fig. 5b). This figure shows how the eastern sector of the Gachsaran Anticline is characterized by two steeply-dipping bounding faults. This sector is characterized by a distinct high uplifted structure on top of the Asmari Formation. Thick sediments of the Miocene Gachsaran evaporites accumulated on both sides of the anticline. Gachsaran Formation as the main upper décollement in the Dezful Embayment clearly decouples the deformation with a syncline filled by Plio-Pleistocene syn-orogenic Aghajari-Bakhtiyari Formations at the eastern sector of the Gachsaran Anticline (Fig. 5b).

4.3. Growth structures above the Gachsaran evaporites

The Gachsaran Formation crops out along the Gachsaran Anticline, whereas the Mio-Plio-Pleistocene Mishan, Aghajari and Bakhtiyari formations are partly preserved in the flanks of this structure. Two broad synclines filled by thick syn-orogenic sediments (Fars Group) bounded the Gachsaran Anticline. However, due to the mobility of the Gachsaran evaporites, the infill of these synclines shows important thickness variations (~100–2000 m) throughout the study area. The synclines flanking the Gachsaran Anticline are characterized by growth strata from the Fars Group with overturned to horizontal attitudes (Fig. 6). These are well preserved in the western sector of the Gachsaran Anticline (Fig. 6a). In the SW flank of this sector, overturned strata of the Gachsaran Formation gradually turn to horizontal in younger deposits of the Bakhtiyari Formation (Fig. 6a). Likewise, the SW flank of the eastern sector of the anticline displays some growth geometries in the Mishan, Aghajari and Bakhtiyari formations (Fig. 6b).

The geometry of the Mishan-Bakhtiyari formations strata in seismic profiles does not match with the subsurface structures below the Gachsaran evaporites due to the mobility of the Gachsaran Formation (Fig. 5). The ductile evaporites tend to flow due to the contractional

Fig. 4. A) Uninterpreted, and B) interpreted clinoform geometries of the Asmari Formation in the SW flank of the Mish anticline. See Fig. 1a for location.

deformation and fill the surrounding basin (e.g. Najafi et al., 2018; Rowan and Ratliff, 2012). However, the geometry and thickness of the Fars Group sediments are important factors since (i) they document the timing of the structure growth; and (ii) thick overburden have an impact on the development of the Gachsaran Anticline. The thickness of overburden sediments directly affects the geometric (e.g. fold vergence) and kinematic (e.g. vertical uplift) evolution of the deep structures (e.g. Barrier et al., 2002; Pichot and Nalpas, 2009; Pla et al., 2019).

4.4. 2D sequential restoration along-strike of the Gachsaran Anticline

A 2D structural restoration of the constructed section (63.5 km long, NW-SE trend) along the Gachsaran Anticline was sequentially established to remove the deformational effects of geological processes such as sedimentation, folding, and faulting in the entire studied area with the primary aim of analyzing the deformation history of the KMF. Restoration of the tectonostratigraphic model reveals how deformation rates evolved through time (Fig. 7). The amount of the eroded sediments (Fars Group) over the topography level was constructed based on the layer geometry as surface outcrops and their preserved thickness in the adjacent areas (~1500 m were constructed) (Fig. 8a). During backstriping, due to the pre-shortening vertical movement of the KMF, a simple vertical shear algorithm (see also Valero et al., 2015) was utilized during the unfaulting and unfolding of the competent rocks and the area balance preservation for the Gachsaran evaporites.

The Mio-Plio-Pleistocene Fars Group reconstructed sedimentary geometry indicate that the strata thickens towards the eastern and western edges of the Gachsaran Anticline from ~1700 m up to a ~2800 m and ~3700 m, respectively (Fig. 7a). This is well demonstrated by the sequential restoration of the Miocene Mishan and Gachsaran formations (Fig. 7b and c). The KMF terminates at the lower portion of the Gachsaran evaporites. However, evidences such as thickness variation and folding of upper layers support that this fault is still active and affect the younger strata. Before restoration at the top of the Asmari Formation, two culminations were detected in both the western and eastern plunges of the Gachsaran structure. These structures were developed during the Mio-Pliocene deposition time of the Gachsaran-Aghajari formations, during the shortening of the Zagros orogeny (Fig. 7b and c). Restoration to the top of the Burdigalian Asmari Formation has removed the effect of both the western and eastern culminations from the entire section profile downward (Fig. 7d). The Oligo-Miocene Asmari and Eocene Pabdeh formations indicate gradual thinning of the strata towards the eastern plunge from~ 1000 up to 600 m in the east of the KMF (Fig. 7d and e). Furthermore, the effect of the KMF on the Asmari Formation geometry is well-documented in the outcrop (Fig. 4).

Sedimentary thickness across the KMF varies from ~1900 to ~300 m depth-wise during the deposition of the Upper Cretaceous Gurpi, Ilam, and Sarvak formations (Fig. 7f and g). The Coniacian-Cenomanian Gurpi Formation was not deposited in the eastern side of the KMF (Fig. 7f). Restoration to the top of the Gurpi Formation reveals gradual thinning of maximum thickness of ~280 m in the western edge of the Gachsaran Anticline towards the east until it pinches out at the west of the KMF (Fig. 7f). However, the thicknesses of the Ilam-Sarvak formations drastically in the east of the KMF where the thick deposits of the Ilam-Sarvak formations (~1100 m) in the west of the Gachsaran Anticline decreases to ~ 200 m on top of the KMF (Fig. 7g). Generally, restoration to the Albian top of the Kazhdumi-Gadvan formations reveals uniform thickness and tectonic inactivity along the KMF. There is only a low-angle tilting, up to a ~1°, of these relatively constant layers towards the west. The relative uniform thickness of this unit shows tectonic quiescence ~100–140 Ma (Fig. 7h–j).

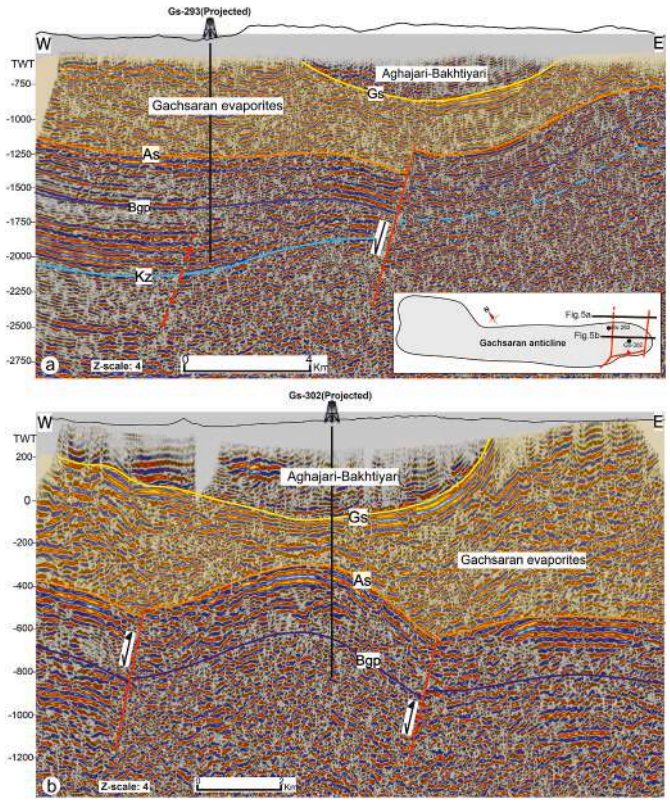

Fig. 5. E-W seismic sections along-strike the eastern sector of the Gachsaran Anticline, a) in the northern syncline, b) over the anticline. The inset map of the Gachsaran Anticline in Fig. 5a shows the location of both sections. Fault slip shown by arrows, discussed in sections 4.4 and 5.1. See location in Fig. 1b. Uninterpreted sections have been provided in Repository data No.2.

4.5. 2D balanced cross-section across the Gachsaran Anticline

The contour map at the top of Oligo-Miocene Asmari Formation of the Gachsaran Anticline indicates changing fold geometry from the eastern to western plunges along the structure (Fig. 1). The map and the constructed cross-sections show that the eastern sector of the Gachsaran Anticline is characterized by a slightly asymmetric angular anticline, and at the western one it is more symmetric. This is related to the activity of the underlying KMF at the eastern sector (Fig. 8a and b, 9a). Figure 9 shows that the two constructed cross-sections on the eastern and western sectors of the Gachsaran Anticline were restored based on the flexural slip algorithm (e.g. Mitra, 2002; Griffiths et al., 2002; Giambiagi et al., 2009). The restored sections are bounded in one end by a pin line that remained straight and perpendicular to the bedding on the restored sections (Fig. 8a and b).

Towards the eastern sector, the fold style varies considerably at the level of the Asmari Formation, in relation with the thickness decreases of the Asmari-Sarvak formations over the KMF (Fig. 8a and b). The eastern fold shows southward vergence with a fault in the southern flank. The different style of the eastern fold in the upper layers is probably related to the folding of the thin Albian to Miocene Sarvak- Asmari formations over the local intermediate décollements of the Albian Kazhdumi and Eocene-Paleocene Pabdeh formations. Low rheologic contrast between Kazhdumi, Sarvak, Pabdeh and Asmari formations over the KMF than that in the western fold made the Kazhdumi and Pabdeh formations more effective décollements in the eastern fold (Fig. 8b). In other words, the activity of the Kazhdumi Formation is a result of thinning of the Asmari-Sarvak formations. The Albian Kazhdumi local décollement in the eastern fold fairly decoupled the upper layer deformation from the below layers resulting in different fold styles in two levels. It is also suggested that the evaporites of the Triassic Dashtak Formation, as the main intermediate décollement in the Dezful Embayment (e.g. Derikvand et al., 2018; Sepehr et al., 2006), was involved in the folding of the both eastern and western folds.

In addition, the cross-section constructed on the western fold presents the Gachsaran Anticline to be a faulted detachment fold. A back-thrust cut the backlimb so that the structure folded over a décollement level uniformly. Balanced cross-sections through the Gachsaran salt-cored anticline show that the asymmetric fault-related folds formed by a transition from faulted detachment fold to fault-propagation folding towards the eastern sector (Fig. 8, e.g. Mitra, 2002). However, the incompetent layers of the Triassic-Jurassic rock units (i.e. the Dashtak Formation), slightly decoupled the deformation in the layers above and below (Fig. 11a). A back-thrust with small displacement probably nucleated at the Dashtak Formation developed in the western sector of the fold (Fig. 11a). In comparison with the eastern sector of the fold, a thicker competent layers of the Paleozoic and Upper Cretaceous Bangestan Group in the western sector of the fold result in a greater fold wavelength (Fig. 8a and b, 9c).

The restoration of the cross-sections in the eastern sector of the fold indicates more shortening in the layers above the Kazhdumi incompetent Formation than that in the below layers (Figs. 8a and 9b). However, more shortening in the sediments over the Dashtak evaporites with respect to the below layers for both structures is deciphered (Fig. 8 a,b). This could indicate that the Gachsaran Anticline is a multi-detachment fold where the deformation mainly affected the upper layers during the shortening of the Zagros orogeny.

As displayed in the cross-sections (Fig. 8) and previous authors (e.g. Abdullahie Fard et al., 2006; Najafi et al., 2018), the Gachsaran Formation is the main upper décollement in the Dezful Embayment, significantly decoupled the structures of the layers above and below. However, it is important to consider the lateral thickness variation of the sedimentary cover as one of the important factors in laterally and vertically changing the fold style in the Gachsaran Anticline.

4.6. Stratigraphic thickness variations, well correlation chart, and isopach maps

Based on the geometry of the strata and the sedimentation rate, the growth strata through the sedimentary profile can be categorized into three intervals (i) the Upper Cretaceous Sarvak-C- Gurpi interval showing the significant thinning/ erosion of the strata towards the KMF, up to 90%; (ii) the Paleocene- Miocene Pabdeh-Asmari interval depicting thinning of the strata up to ~50%, and (iii) considerable growth of the strata, decreased from ~3700 to 1700 m (~55%), during the deposition of the Mio-Plio-Pleistocene Fars Group. Based on numerous well data (~ 400 that drilled up to the Kazhdumi Formation) six isopach maps are constructed from the Sarvak to Asmari formations. (Fig. 10). Isopach maps reveal the tectonic effect on the basin. These maps display how the thicknesses of the Asmari and Pabdeh formations from the western to eastern plunges of the Gachsaran Anticline, over ~70 km of distance, decrease from ~530 m to 240 m and 230 to 120 m, respectively. However, the maps of the Sarvak-B, Sarvak-C, Ilam, and Gurpi formations do not show any deposition in the eastern plunge of the anticline (Fig. 10b). These variations is related to the most severe stage of non-deposition/erosion over the KMF which began from the late Cenomanian to the Maastrichtian time. Reactivation of the pre-existing structures in the late Cretaceous is one of the well documented tectonic activity in the foreland of the Zagros Orogen (see also Abdullahie Fard et al., 2006, Shamszadeh et al., 2022).

A section parallel to the fold axis of the Gachsaran and Dara anticlines and across the KMPH constructed by 17 drilled wells demonstrates the impact width of the KMPH on the sedimentary cover (Fig. 11). This section also shows the considerable impact of the KMPH on the Late Cretaceous sediments where huge non-deposition/erosion occurred on the eastern sector of the Gachsaran Anticline (Figs. 10

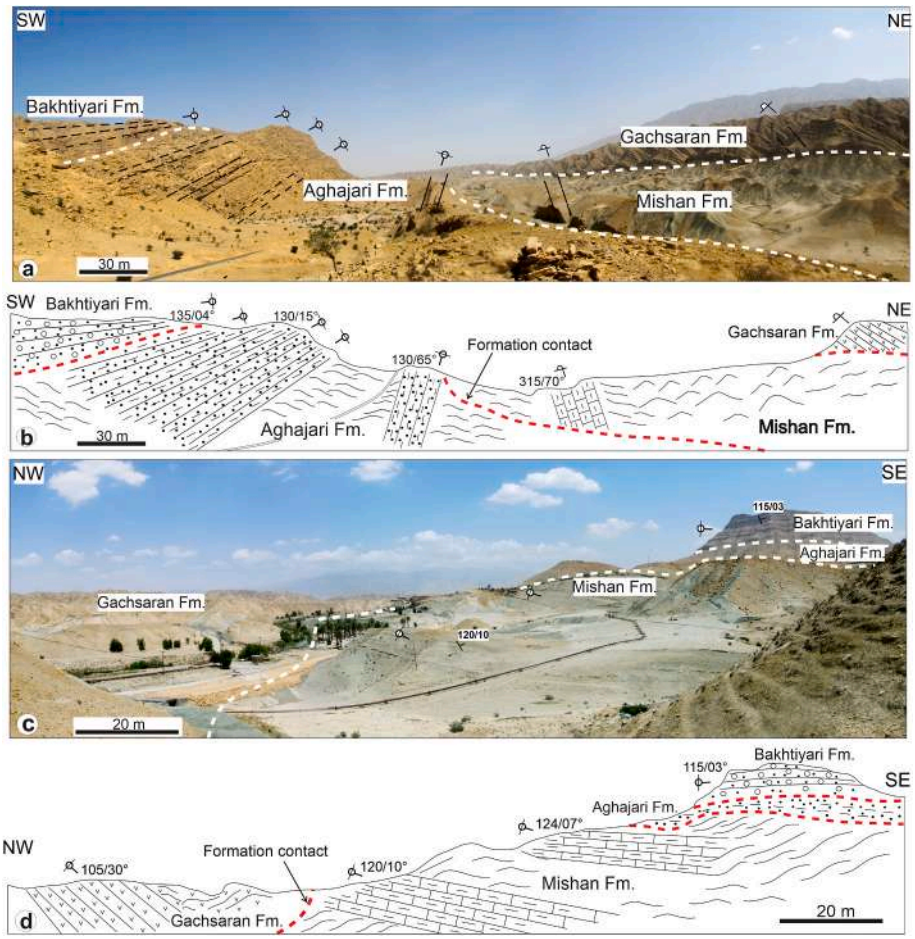

Fig. 6. Field views of the outcropping out rocks at the western (a) and the eastern sector; (b) of the Gachsaran Anticline. Figures (b) and (c) are the line drawing of figures a and c, respectively. Note the different dip attitudes of the Aghajari-Bakhtiyari formations and the overturned beds of the Gachsaran and Mishan formations show in the SW flank of these structures. White/red dashed lines correspond to the formation boundaries. See location in Fig. 1b. (For interpretation of the references to colour in this figure legend, the reader is referred to the Web version of this article.)

and 11). In the section, the Sarvak Formation is divided into three zones including Sarvak-B, C and D (Fig. 11). From Sarvak-D up to the Gurpi Formation only the Sarvak-D has been detected in the eastern sector of the anticline. Based on the well correlation chart (Fig. 11) and geometry of the strata (Fig. 3b), it is assumed that the Sarvak-C and D units are pre-growth strata subject to erosion. The erosional surface occurred on top of the Sarvak-C and Sarvak-D units as the growth strata of the Sarvak-B, Ilam, and Gurpi formationspinch outs and never lie atop the eastern sector of the structure.

Further, the erosional surface is onlapped by the growth strata of the Pabdeh Formation at the top of the eastern sector of the structure (Fig. 11). Few regional studies have detected an erosional surface in the Ilam-Sarvak interval on top of the Hendijan-Bahregansar paleo-high (e.g. Abdullahie Fard et al., 2006; Riahi et al., 2021). This regional unconformity and sharp thickness variation date back to the latest Turonian (~90 Ma) ophiolite obduction in the NE of the Afro-Arabian plate (e,g, Alavi, 2007; Orang and Gharabeigli, 2020). In the Hith- Kazhdumi rock package, sediment thickness is almost constant from the western to the eastern sectors of the Gachsaran Anticline (Fig. 11). The relative uniform thickness of these formations may be related to a period of tectonic quiescence at the deposition time (uppermost Jurassic-Albian).

5. Discussion

Based on several studies, in the fold and thrust belts, the greater thickness of the sedimentary cover has great importance in further propagation of fault-related fold structures toward the foreland than the area with thinner sedimentary cover (e.g. Farzipour-Saein et al., 2013; Marshak and Wilkerson, 1992). In addition, researchers have investigated the effect of mechanical behavior and thickness of the sedimentary cover on the fold style and geometry (Motamedi et al., 2012; Najafi et al., 2014; Sepehr et al., 2006). The 3D view of the Gachsaran Anticline (Fig. 12) and the amount of the shortening (Figs. 8 and 9b) indicate the further propagation towards the foreland occurs in the western sector of the fold, where the sedimentary cover is thicker (Fig. 12). Along-strike differential shortening was accommodated by ~200 m left-lateral strike-slip movement along the KMF (a branch of the deep-rooted KMF in the sedimentary cover) (Fig. 12). The compressional regime of the ZFTB resulted in the reactivation of the inverted KMF as a tear fault in the sedimentary cover. In fold and thrust belts, tear faults develop due to along-strike variation in structural style and differential displacement between two adjacent areas (e.g. Duffy et al., 2018; Pash et al., 2020). During the contraction, the developed tear fault sub-parallel to the Zagros shortening direction accommodates different deformation styles between the eastern and the western sectors of the Gachsaran Anticline (Fig. 12). Therefore, the strike-slip movement along a KMF branch could be attributed to the variable thickness of the sedimentary cover and different propagation between two areas rather than totally originated by the pre-existing deep-rooted KMF (Fig. 12).

5.1. Inversion tectonics adjacent to the KMF

Several studies have emphasized that the inverted compressional structures are strongly controlled by the pre-existing normal fault attitude and direction of the stress field (e.g. Del Ventisette et al., 2006; Deng et al., 2021; Letouzey et al., 1990). In addition, different deformation phases related to reactivation of inherited faults have been considered in several tectonic settings worldwide (e.g. Cooper and Williams, 1989; Dasgupta and Mukherjee, 2017; Riahi et al., 2021; Tari et al., 2020). Change in tectonic regime from extension to contraction

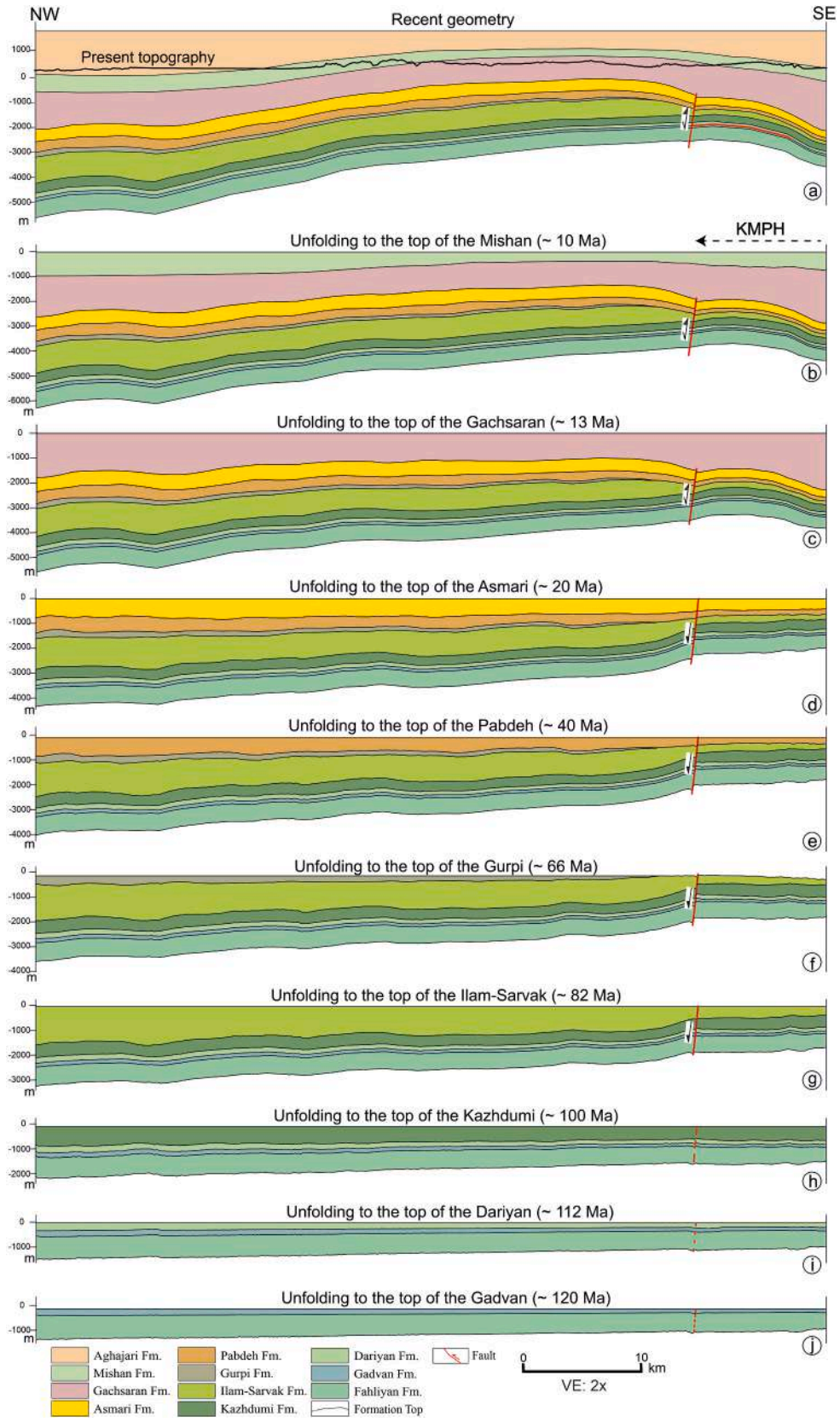

Fig. 7. 2D sequential restoration along strike the Gachsaran Anticline crossing the Kharg-Mish Paleo-high from top of the Gadvan Formation to recent sediments. The present topography (black line) is taken from the Digital Elevation Model (DEM) map (10 m spatial resolution) of the study area. KMPH: Kharg-Mish Paleo High. See Fig. 1b for the section location.

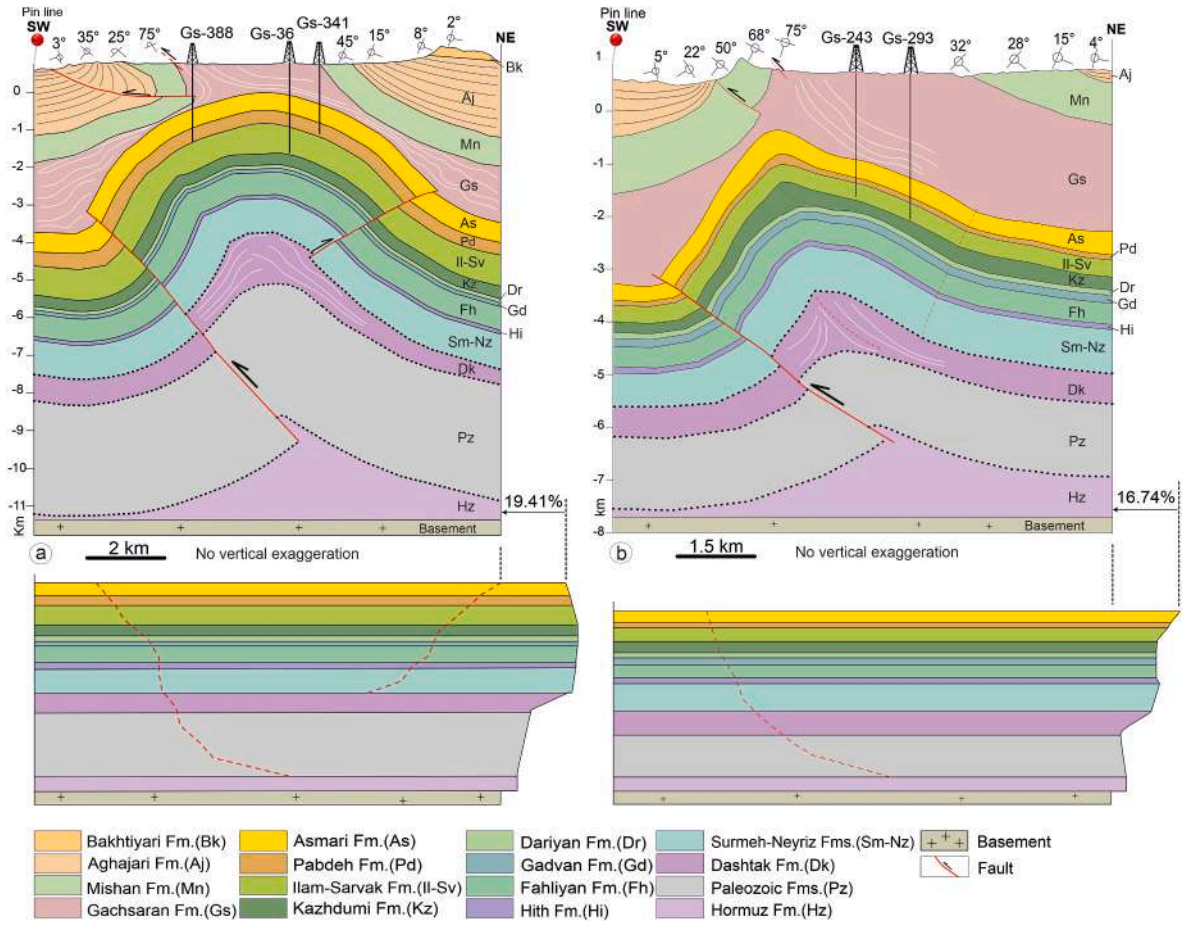

Fig. 8. Two constructed balanced cross-sections on the Gachsaran Anticline, across the western (a) and the eastern sectors (b). See Fig. 1b for location.

has been considered along the pre-existing extensional KMF in the eastern sector of the Gachsaran Anticline. The effect of the KMF reactivation on the thickness and facies variation of the Late Cretaceous sediments were mentioned by the previous workers (e.g., Karimnejad Lalami et al., 2020; Motiei, 1995; Sherkati and Letouzey, 2004). Further, several researchers investigated the reactivation and multiphase deformation of the N-S basement faults in tectonic-sedimentary evolution and kinematics of the South Dezful Embayment (e.g. Abdullahie Fard et al., 2006; Riahi et al., 2021; Shamszadeh et al., 2022). However, in this research, based on sequential restoration and unfaulting of the different horizons interpreted from seismic and well data, displacement and style of inversion tectonics along the KMF have been quantified (Fig. 13). The KMF, a long-term active tectonic structure in the eastern sector of the Gachsaran Anticline, controls the depositional basin of the area. The multiple reactivations of this fault have controlled the sedimentary variation along-strike of the Gachsaran Anticline at least from Late Cretaceous times.

Several studies utilized the geometry of the syn-tectonic sediments to analyze the tectonic history of the growth structures (i. e. faults and folds) (e.g. Castelltort et al., 2004; Deng et al., 2021; Storti and Poblet, 1997). The amounts of the heave, dip separation, and throw of the fault have been calculated during the Aptian (~115 Ma) to Pliocene (~2-5 Ma) time (Fig. 13). For the graphical display of the fault analyses, we used the plot of cumulative dip separation on each horizon vs. time. Similar plots have been presented by McClymont et al. (2009) and Koukouvelas et al. (2017). We use this plot in analyzing the growth fault kinematics from the back-stripping method for the tops of the Asmari, Pabdeh, Sarvak, Kazhdumi and Dariyan formations (Fig. 13f). Displacement profiles for each horizon display the systematic accumulation of the fault slip from Aptian (~115 Ma) to Pliocene (~2–5 Ma) times (Fig. 13a–e). The value above the zero (reference line) indicates existing normal dip separation on each horizon at a specific time. Conversely, the value below zero indicates the existing reverse dip separation on each horizon. Where the curves are on the reference line it means the dip separation amount of the normal and reverse faulting are equal in this specific time. The plot indicates that the contractional tectonic inversion occurs in the Burdigalian where the slope of curves changes downwards (Fig. 13).

Two major faulting episodes with different mechanisms in the Cenomanian and Pliocene have been recognized. Major normal faulting in the Cenomanian (Fig. 13b) was followed by a period of slight normal faulting until Pliocene (Fig. 13c and d). In the Pliocene, a significant reverse dip separation occurred along the fault, which is probably related to the oblique contraction of the Zagros orogeny (Fig. 13e). The pre-existing structures/extensional basement faults in the external parts of the foreland in an orogenic belt could be reactivated in response to the plate margin's stress, flexure produced by the orogen (e.g. Ziegler et al., 1995).

Positive inversion along the KMF has developed a culmination and partly uplifted the horizons on the western side (hanging wall) of the fault (Fig. 13e). In such an inversion, the horizons on both sides of the faults may show normal displacement in lower horizons and reverse slip in the shallower levels (e.g. Coward, 1994; McClay, 1989; Cooper and Warren, 2020). Figure 13f shows the values of cumulative dip separation of the horizons across the KMF from Aptian up to Pliocene times. Currently, reverse separation values (negative values) only are visible on the Asmari and Pabdeh formations at the end of the multiple activity of the fault (Fig. 13f).

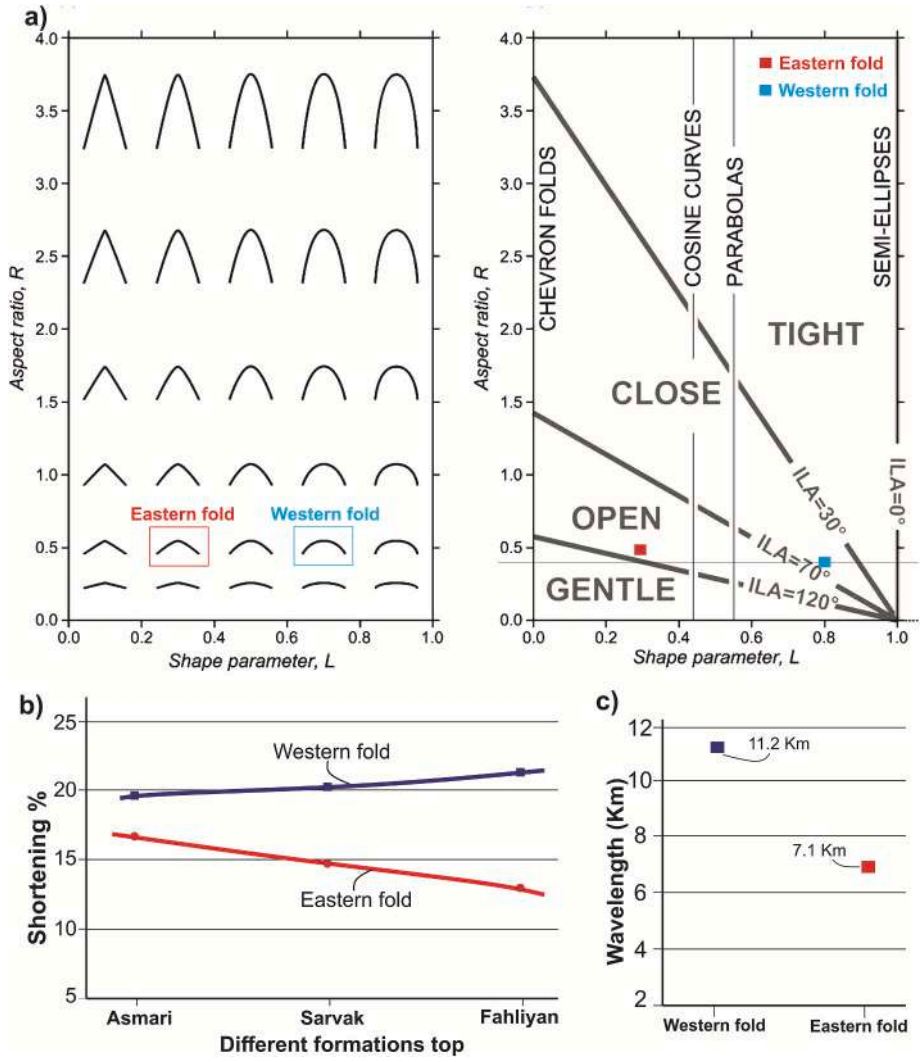

Fig. 9. Fold classification based on the aspect ratio, shape parameters, and interlimb angle (ILA) for the eastern and western folds on top of the Asmari Formation. (see Srivastava and Lisle (2004) for the method and parameters calculation). b) Plot of different amounts of shortening on top of three formations of Asmari, Sarvak, and Fahliyan for both eastern and western folds. C) Diagram shows different wavelengths of the western (11.2 km) and eastern (7.1 km) folds in the Asmari Formation.

5.2. Depth of detachments in the Gachsaran Anticline

Several researchers attributed various incompetent evaporite and shale units in the sedimentary cover, which may act as décollement for the structures of the Dezful Embayment (e.g., Derikvand et al., 2018; Sherkati and Letouzey, 2004). In the Gachsaran Anticline, the mechanical behavior of the sedimentary succession varied the fold style laterally and vertically. The constructed cross-sections across the anticline show several incompetent units viz., Hormuz evaporites, Dashtak evaporites, Kazhdumi and Pabdeh shales and Gachsaran evaporites as decollement levels. These played important roles during the shortening and structural evolution (Fig. 8a and b). The role of the local decollements (Pabdeh and Kazhdumi formations) in the eastern sector is more significant where the competent rocks thin. Because of poor quality seismic data at depth, the presence of Hormuz salt as a basal décollement is still uncertain. Hence, the main décollement level for the subsurface anticlines in the Dezful Embayment is still debated. However, several researchers attributed the Dashtak Formation as a major detachment level that controlled the overlaying folds up to the Gachsaran Formation (e.g. Asgari et al., 2019; Derikvand et al., 2018; Sherkati et al., 2006). In addition, a few studies have considered the Hormuz salt or its equivalent as the main décollement controlling overlying folds up to the Gachsaran evaporites in the Dezful Embayment (e.g. Beauchamp et al., 2000; Carruba et al., 2006; Heydarzadeh et al., 2020).

Open and rounded fold geometries as well as the development of a footwall syncline in the Gachsaran Anticline indicate that such a fold is probably developed above a strong décollement horizon as a faulted detachment fold structure (Figs. 8a and 9a). However, variations in the thickness of competent and incompetent units and depth of the detachment can impact the geometry of the fold and fault (Dahlstrom, 1990; Farzipour-Saein and Koyi, 2016; Sepehr et al., 2006). In addition, the relationship between fold wavelength and depth of the detachment has been noted (e.g. Casciello et al., 2009; Derikvand et al., 2018; Sepehr et al., 2006).

Calculation of detachment depth is an essential method to construct, balancing and restoring cross-sections in fold-and-thrust belts (Bulnes and Poblet, 1999; Epard and Groshong, 1993). To calculate the main detachment level of the western and eastern folds of the Gachsaran Anticline, we use the computational (Chamberlin, 1910) and graphical methods (e.g., Bulnes and Poblet, 1999; Epard and Groshong, 1993). Based on the area-conservation principle, the Chamberlin method takes a specific folded horizon to calculate its underneath excess area that is equal to the detachment depth. However, having the amount of shortening and excess area it is possible to calculate the depth of the

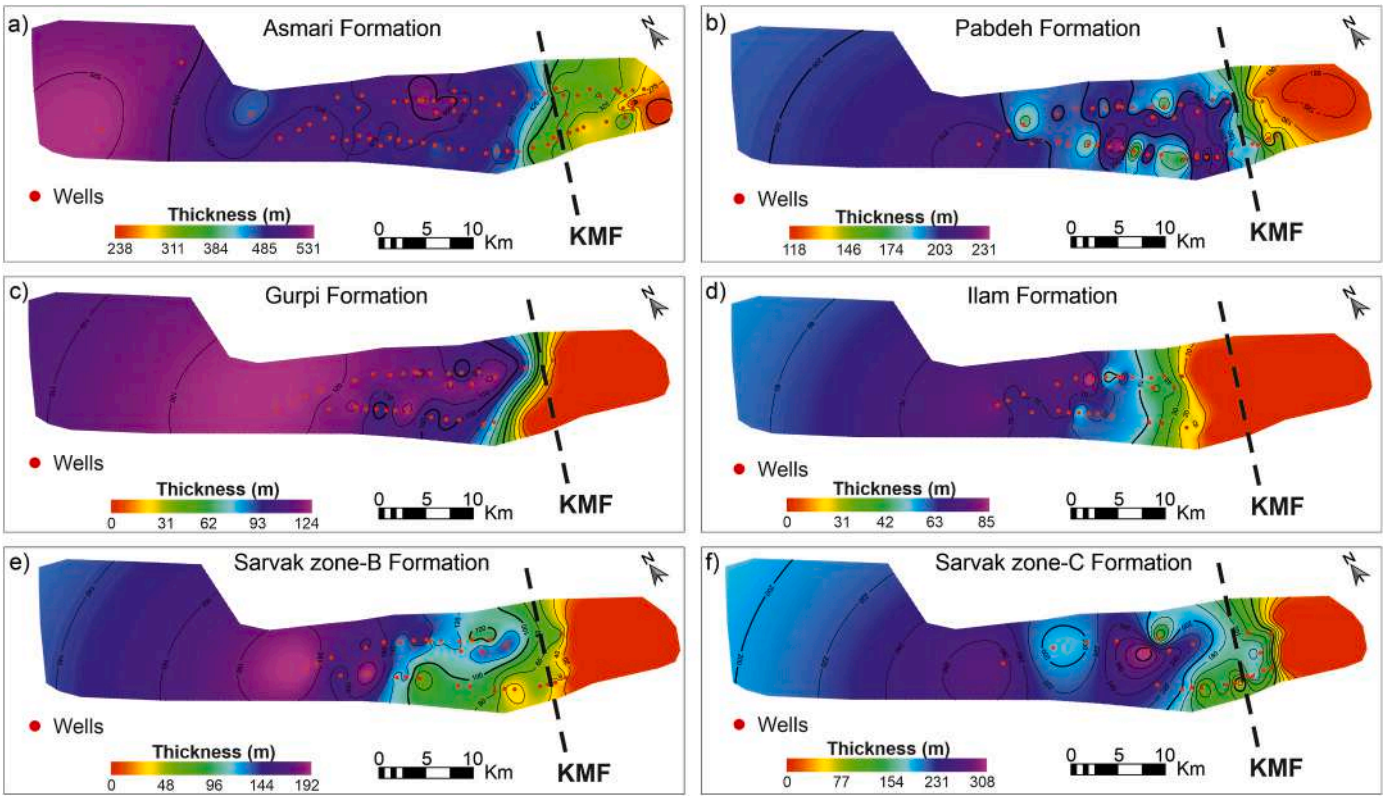

Fig. 10. Isopach maps of the Gachsaran Anticline from the Miocene Asmari Formation (a) up to the Upper Cretaceous Sarvak Formation (f). The dashed black line shows the approximate trace of the KMF. True Stratigraphic Thickness (TST) was considered to construct the thickness maps.

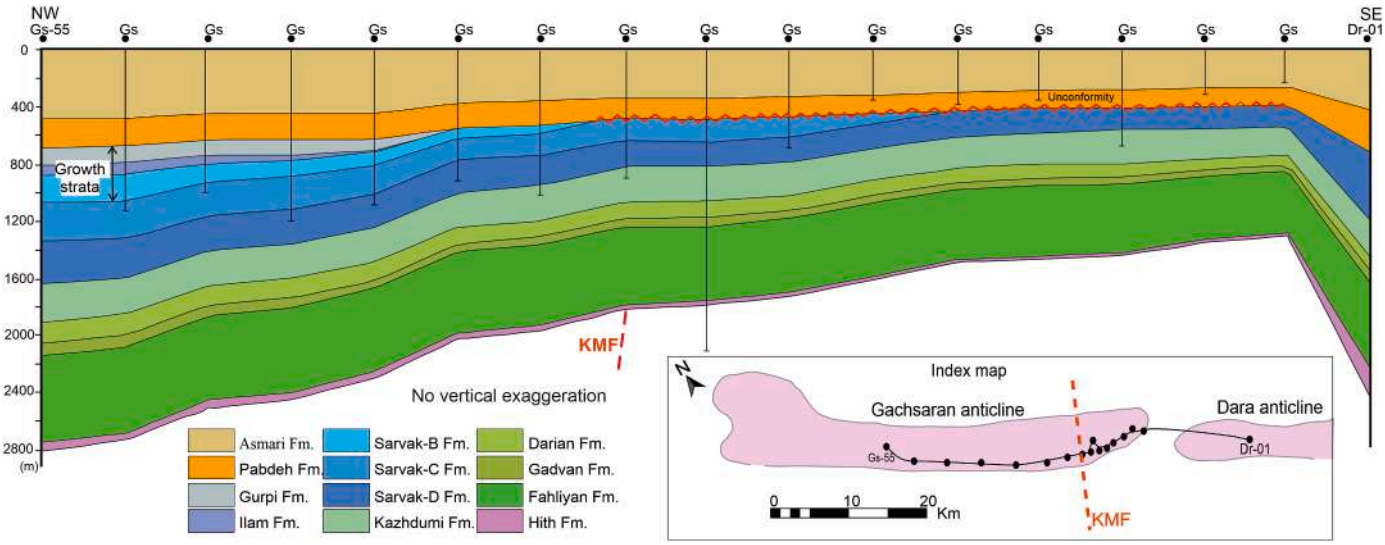

Fig. 11. Well-correlation section along-strike the Gachsaran and Dara anticlines and across the KMF. See Fig. 1a for the location.

detachment horizon.

The detachment depths have been calculated for the Sarvak, Dariyan, Fahliyan and Surmeh formations in the eastern and western folds using the Chamberlin method (Table 4). The tops of these formations have been considered as reference level/regional datum to avoid the effect of upper incompetent layers, e.g. Kazhdumi and Gachsaran formations (Fig. 14). The calculated detachment depths were used in the graphical plot (Fig. 14) as per Bulnes and Poblet (1999).

Based on this method ~10,150 m and 13,300 m depth are calculated for the eastern and the western folds of the Gachsaran Anticline, respectively (Fig. 14). Despite the effect of the two intermediate décollement levels (i.e. Dashtak and Kazhdumi formations) on the fold style of the upper layers, the Gachsaran Anticline is mainly developed and originated over the lower main décollement of the Hormuz series, which decoupled the sedimentary cover from the gneissic basement. An approximate difference of 3000 m in detachment depth between eastern and western folds indicates the possible uplift of the basement block in the eastern sector of the Gachsaran Anticline. The constructed balanced cross-sections (Fig. 8) demonstrate a significant relationship between the wavelength and style of folds with depth to detachment horizon.

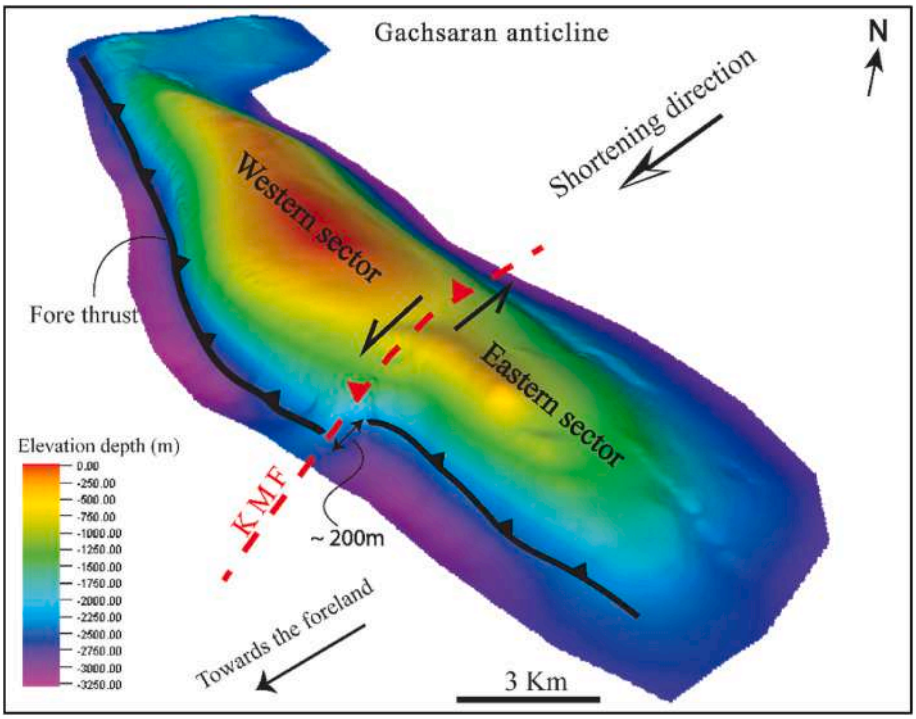

Fig. 12. 3D view of the Gachsaran Anticline at the top of the Asmari Formation indicates different degrees of deformation between the eastern and western sectors that are accommodated by a sub-vertical left-lateral strike-slip fault. KMF: Kharg-Mish Fault.

5.3. *Fracture density in the Gachsaran Anticline*

Fractures play an important role in reservoir enhancement and hydrocarbon migration. Limestone reservoirs of the Upper Cretaceous Bangestan Group (Sarvak and Ilam formations) in the ZFTB are mainly known as the carbonate fractured reservoirs (e.g. Kosari et al., 2017; Soleimani et al., 2017). According to the low porosity of this reservoir in the study area, ~2.2%, the role of fracturing is significant in the increase production. A general map view of the fracture intensity throughout the Gachsaran oilfield from a constructed Discrete Fracture Network (DFN) model using Petrel software (2016) has been presented (Fig. 15). The model involves the following data: production and well test data, mud loss, image logs and core data from ~400 drilled wells (not all reached to the Bangestan Group) covering the Gachsaran Anticline. Construction of the DFN model is a multi-step procedure involving different techniques in reservoir modeling and simulation (e.g. Fang et al., 2017; Yaghoubi, 2019). A map view of the average fracture density map of the Upper Cretaceous Bangestan Group demonstrates moderate to high fracture density adjacent to the KMF (Fig. 15). However, the fractures are less developed in other parts of the field. The high fracture density adjacent to the KMF could be related to three factors: (i) these fractures are related to the deep-rooted fault reactivation of the KMF during the Late Cretaceous ophiolite obduction, (ii) the interaction zone between two eastern and western sectors of the Gachsaran structure with different amounts of shortening produced tear fault with associated high fractured zone, and (iii) in the Ilam-Sarvak formations the fracture intensity could be enhanced by uplift and erosion (e.g. DiBiase et al., 2018; Narr and Currie, 1982).

5.4. *Conceptual evolutionary structural model of the Gachsaran Anticline*

Overprinting of the Zagros deformation front on several pre-existing basal structures (e.g. salt wall, basement faults) was accommodated by inversion and reactivation of basement faults and squeezed salt structures (e.g. Jahani et al., 2017; Rowan et al., 2022; Santolaria et al., 2021; Talbot and Alavi, 1996). The results of this article, supported by previous studies, suggest a conceptual model with six steps to illustrate the structural evolution of the Gachsaran Anticline (Fig. 16) including:

(a) Late Proterozoic-Early Cambrian Hormuz salt deposited over a series of horst and graben basement structures (e.g. Edgell, 1992; Husseini, 1988; Stewart, 2018). The basement architecture controlled the differential thickness of the Hormuz salt throughout the area (e.g. Jahani et al., 2017; Talbot and Alavi, 1996) (Fig. 16a).

(b and c) Basement fault reactivation and Early Paleozoic salt movement followed by the Hercynian orogeny during the Carboniferous developed many salt-cored structures (or probably salt stock) mainly along the NNE-SSW trending basement faults in the NE of the Arabian plate (e.g. Faqira et al., 2009; Stewart, 2018). Along with the Kharg-Mish Fault trend, several salt-cored anticlinal structures such as the Dorood, Berris and Hasbah fields developed in offshore (Fig. 1). The subsurface data in the NE of the Arabian plate indicate considerable erosion/or non-deposition of the pre-Hercynian sediments across the NNE-SSW trending basement structure (Faqira et al., 2009; Stewart, 2018) (Fig. 16b and c). In the eastern sector of the Gachsaran Anticline, poor quality seismic data at depth makes difficulty in the interpretation this event (see also Shamszadeh et al., 2022). However, based on the result of this study the evidence such as depth to basal detachment and small wavelength of the eastern sector fold, thinner Paleozoic competent rocks over the KMF look plausible.

(d) After a period of relative tectonic quiescence, Late Cretaceous ophiolite obduction in the NE of the Arabian margin reactivated the pre-existing basement structure e.g., Kharg-Mish fault, further towards the foreland (e.g. Bahroudi and Talbot, 2003; Orang and Gharabeigli, 2020). Huge erosion/or non-deposition of the Sarvak-Gurpi formations have documented this well-known tectonic event throughout the Dezful Embayment and the Persian Gulf (Fig. 16d).

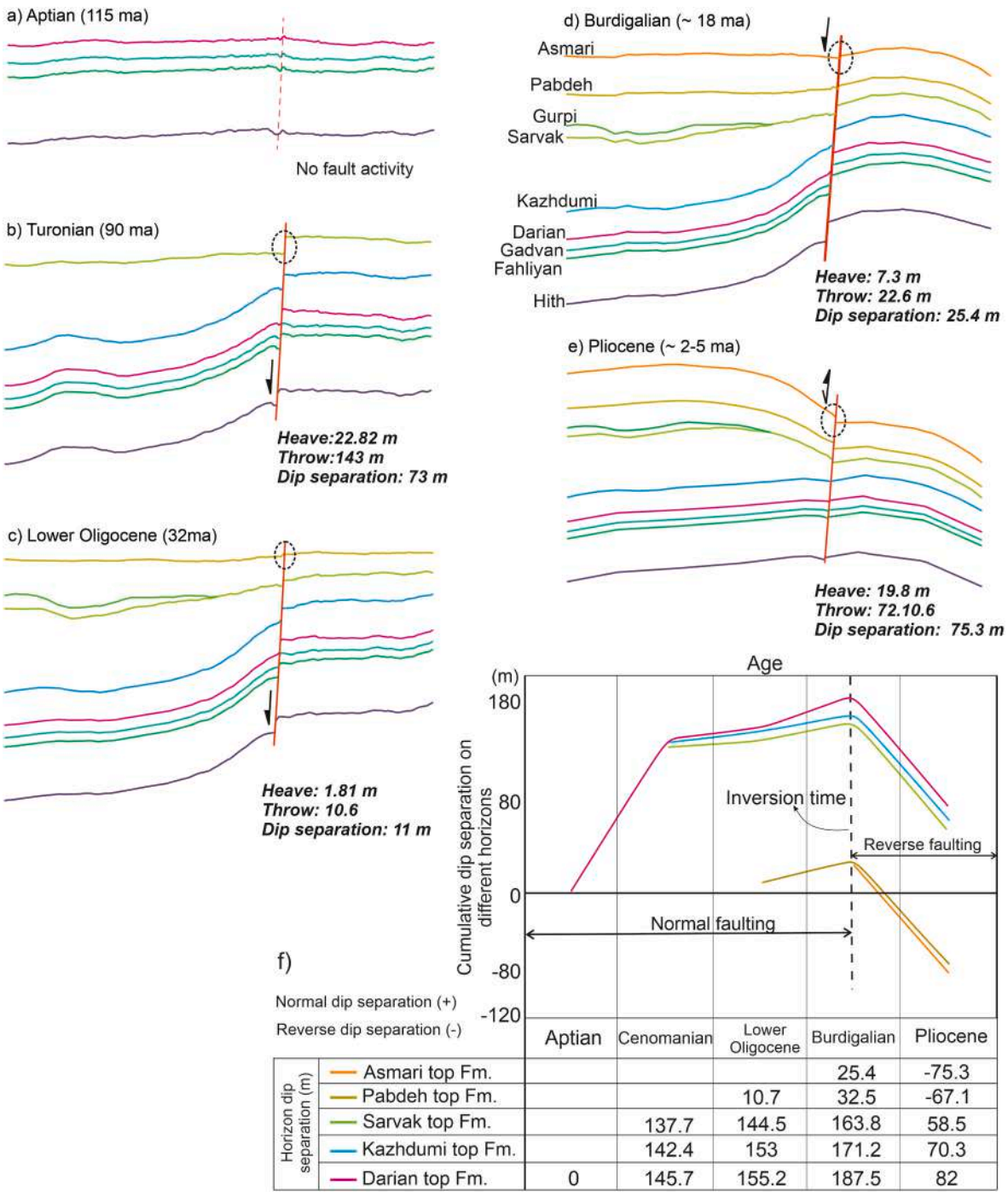

Fig. 13. The numerical analysis of the KMF crossing the eastern sector of the Gachsaran Anticline over time, a) Aptian (~115 Ma); b) Cenomanian (~95 Ma); c) Lower Oligocene (~32 Ma); d) Burdigalian (~18 Ma); e) Pliocene (~2-5 Ma) time.

(e) Sequential restoration results and thickness variation along-strike of the Gachsaran fold axis indicate that the eastern sector of the anticline developed early. During Oligo-Miocene, the Asmari-Pabdeh formations thinned gradually towards the east of the structure (Fig. 16e).

(f) The Fars Group growth strata documented in outcrop and seismic profiles show the intense growth of the Gachsaran Anticline since Late Miocene. Thicker sedimentary cover in the western plunge of the Gachsaran Anticline than the eastern plunge (over the KMF) produced a broad anticline with a large wavelength towards the west (Fig. 16f). Additionally, differential shortening along-strike of the Gachsaran Anticline is accommodated by tear faulting between two areas with different propagation fronts into the foreland (Fig. 16f).

6. Implications for hydrocarbon exploration

The anticlinal reservoirs are structurally complex, especially when the structure developed over a pre-existing reactivated fault zone. Several studies have emphasized the influence of pre-existing basement structure on hydrocarbon migration and accumulation in the NE of the Arabian plate (e.g. Baniasad et al., 2021; Beydoun, 1991). Reactivation of pre-existing structures could re-migrate and trap hydrocarbon. Besides, repeated reactivation of the basement faults placed the source,

Table 4
Depth of the detachment calculation and parameters utilized for the Eastern and Western folds of the Gachsaran structure obtained with the method proposed by Chamberlin (1910).

Section	Formation	Unfolded bed length (L_0), m	Deformed bed length (w), m	Shortening (s), L_0-w	Excess area (A_t) m^2	Detachment depth (z) = A_t/s, m	Depth of regional datum, m
Western fold	Sarvak	15,133.2	12,045.8	3087.4	23,482,658.4	7606	−4400
Western fold	Dariyan	15,296.89	12,045.8	3251.09	22,969,610.6	7065	−5650
Western fold	Fahliyan	15,288	12,045.8	3243	22,097,585	6813	−5850
Western fold	Surmeh	15,252	12,045.8	3207	19,987,135	6232	−6570
Eastern fold	Sarvak	11,175.8	9508.1	1667.7	10,502,235	6300	−3250
Eastern fold	Dariyan	10,922.8	9508.1	1414.8	8,179,715.6	5781	−3700
Eastern fold	Fahliyan	10,957	9508.1	1449	7,885,622.6	5442	−4060
Eastern fold	Surmeh	10,850	9508.1	1342	7,011,109	5224	−4560

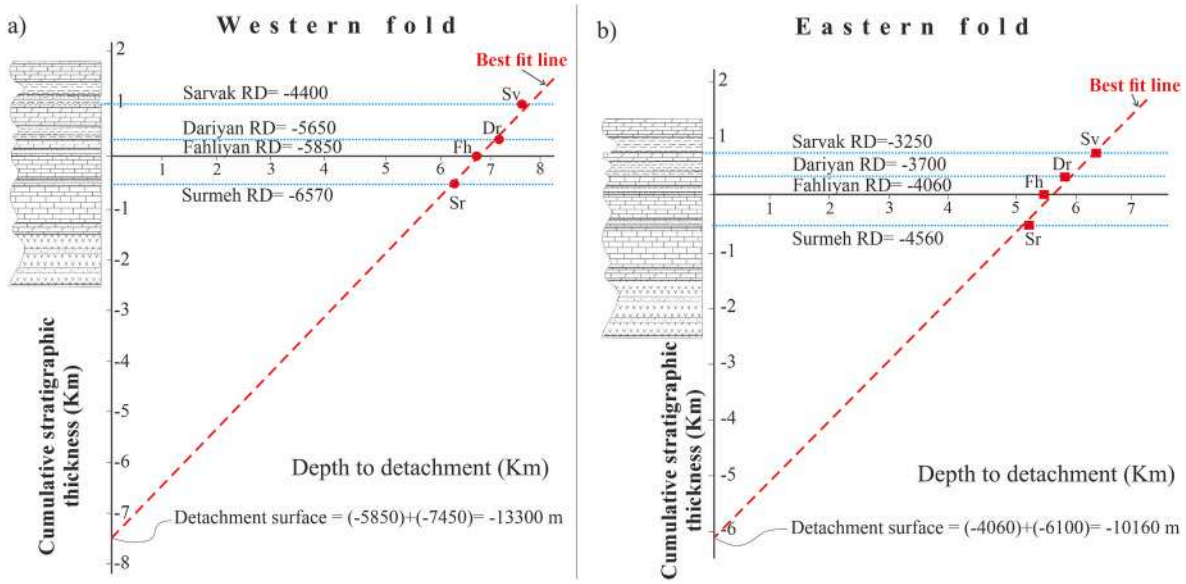

Fig. 14. Detachment depth calculation of the western (a) fold and eastern fold (b) of the Gachsaran Anticline for the Sarvak (Sv), Dariyan (Dr), Fahliyan (Fh), and Surmeh (Sr) top formations horizons obtained by the method proposed by Bulnes and Poblet (1999). RD: Regional datum.

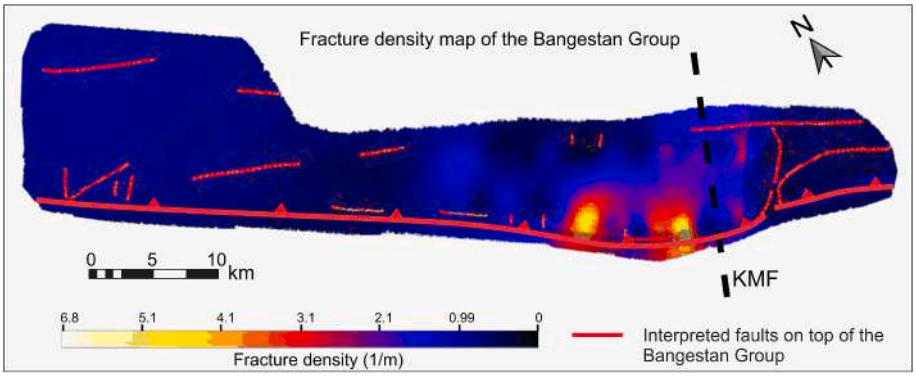

Fig. 15. The fracture density map of the Bangestan Group shows a moderate to high-density fracture zone adjacent to the Kharg-Mish Fault. The map shows the Gachsaran Anticline at the depth of the Bangestan Group. See Fig. 1 for location.

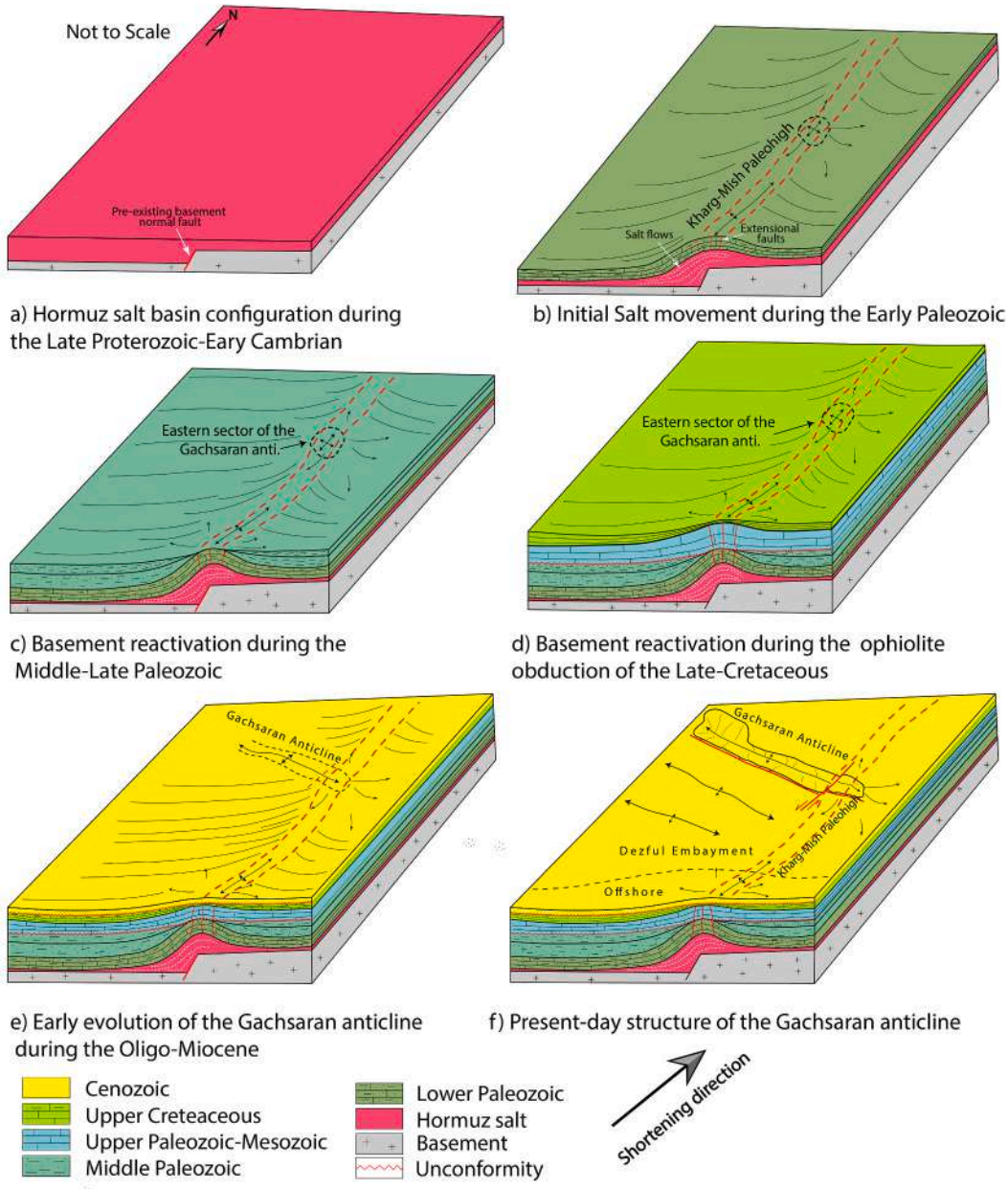

Fig. 16. 3D conceptual block showing the structural evolution of the Gachsaran Anticline related to the Kharg-Mish paleo-high.

trap and seal rocks at different stratigraphic levels (e.g. Bahroudi and Talbot, 2003). In other words, positive inversion tectonics along the pre-existing faults results in the developed steep reverse faults and complex structures in the sedimentary cover. This might impact the sealing properties (e.g. Buchanan and Buchanan, 1995; Cooper and Williams, 1989; Holdsworth et al., 1997; Riahi et al., 2021).

Based on the back-striping results, during the Late Cretaceous inversion tectonics the eastern sector of the Gachsaran Anticline placed at a higher level. This sector of the anticline first started folding, which is important to consider in terms of hydrocarbon migration and entrapment. Persuming hydrocarbon migration since the Late Miocene (e.g. Bordenave and Hegre, 2005; Baniasad et al., 2019; Vatandoust et al., 2020), the eastern sector of the Gachsaran Anticline, over the N-S trending KMF, is a potential site for the accumulation of a large share of hydrocarbons. Generally, it could be said that the structures over the KMF may have a lower hydrocarbon exploration risk.

However, note the negative impact of the KMF on the rock volume of the Upper Cretaceous Bangestan reservoir, where large erosion/or non-deposition decreases its thickness to ~10% of the total.

Long-term fault activity and localization strain in the eastern sector could have fractured/enhanced the reservoirs. Based on the porosity and permeability of the Asmari reservoir in the Dezful Embayment were enhanced by fractures related to the basement fault reactivation (e.g. McQuillan, 1991; Al-Hajeri and Bowden, 2017; Al-Hajeri et al., 2017).

7. Conclusions

Through this study, we establish a tectonic connection between pre-existing deep-seated fault and contractional deformation in the sedimentary cover during the evolution of the Gachsaran Anticline. The N-S deep-seated KMF across the eastern sector of this anticline, as a location of heterogeneity or weakness, localized the deformation during the Zagros orogeny. Consequently, the growth strata of the Late Cretaceous deposits and Mio-Plio-Pleistocene Fars Group show that the Gachsaran Anticline at first started growing from the east and developed towards the west.

Kinematic analyses of the KMF in the eastern sector of the Gachsaran Anticline are attained by Aptian-Pliocene activity of normal and reverse faulting. After a relative tectonic quiescence between Barremian-Cenomanian times, the reactivation of the KMF with normal faulting in the Turonian led to the huge erosion/non-deposition in the Late Cretaceous (Sarvak, Ilam and Gurpi formations) on the eastern side of the fault. Normal faulting accompanied with gradual thinning of the Paleocene-Oligocene deposits (Pabdeh-Asmari formations) continued until the Burdigalian. During the Pliocene, a significant reverse slip probably related to the contraction of the Zagros orogeny occurred along the fault. Positive inversion along the KMF has developed a culmination and partly uplifted the western sector of the anticline.

Structural evolution of the Gachsaran Anticline is divided into three main stages: 1) reactivation of the KMF in the Turonian in response to obduction of the Neyriz and Kermanshah ophiolites in the suture zone of the ZFTB, which uplifted the eastern sector of the Gachsaran Anticline probably with an N-S axial trace; 2) growth strata developed in Late Cretaceous – Miocene times towards the KMF possibly related to slight continuous uplift of the eastern secor; and 3) rapid folding and uplift (mainly in the western sector) in the Post-Miocene due to the main Zagros orogenic pulse. This is supported by the thick syn-orogenic Fars Group sediments and positive inversion along the KMF.

The thin sedimentary cover in the eastern sector of the Gachsaran Anticline produced a fold with a smaller wavelength and styles different from the western sector. In other words, the different depth of the basal décollement layer along the structural trend of the Gachsaran Anticline controls the geometry of the fold during the contractional deformation.

Complex structural evolution in the eastern sector of the Gachsaran Anticline along with a higher fracture intensity, and well production adjacent to the KMF are factors to consider for future exploration activities along the KMPH.

Declaration of competing interest

The authors declare that they have no known competing financial interests or personal relationships that could have appeared to influence the work reported in this paper.

Data availability

Data will be made available on request.

Acknowledgments

We thank the National Iranian South Oil Company (NISOC) for providing the Seismic and well data and permission to publish this article. This study is a part of the Ph.D. thesis of AS supported by the Shiraz University Research Council (SURC) grant. Cumulative Professional Development Allowance (Indian Institute of Technology Bombay) supported SM. OF acknowledge the support of the research project Structure and Deformation of Salt-bearing Rifted Margins (SABREM), PID 2020-117598 GB-I00, funded by MCIN/AEI/10.13039/501100011033. Innovación" of the Spanish government and by Statoil. Schlumberger and Midland Valley are also acknowledged for providing Petrel (2016) and Move software (2018) respectively. Associate Editor Prof. Alexander L Peace. and reviewers (Dr. Jennifer Aschoff, Dr. Victor Alania, and three anonymous persons) are thanked for providing detailed comments.

Appendix A. Supplementary data

Supplementary data to this article can be found online at https://doi.org/10.1016/j.marpetgeo.2022.105871.

Appendix

Abbreviations

Aj	Aghajari
BH	Bibihakimeh
BGP	Bangestan Group
Bk	Bakhtiyari
BFZ	BalaRud Fault Zone
D	Dorood oilfield
Dr	Dara anticline
Eq	Equation
Fm	Formation
Fh	Fahliyan Formation
Gd	Gadvan Formation
Gs	Gachsaran
HBPH	Hendijan-Bahregansar Paleo High
Hi	Hith Formation
HPH	HellehPaleo High
HT-LP	High Temperature- Low Pressure
HP-LT	High Pressure- Low Temperature
IFZ	Izeh Fault Zone
KMF	Kharg Mish Fault
KMPH	Kharg Mish Paleo High
KZF	Kazerun Fault Zone
Kz	Kazhdumi Formation
MFF	Mountain Front Flexure
SDE	South Dezful Embayment
RD	Regional Datum
Sr	Surmeh Formation
TWT	Two-Way Travel time
UDVA	Uromieh-Dokhtar Volcanic Arc
ZFTB	Zagros fold-and-thrust belt

Symbols

c	Porosity/depth coefficient
A	Displaced area
z	Depth
l	Length
w	Fold width
s	Shortening
f_0	Surface porosity
f	porosity
l_0	Initial bed length
A_t	Excess area

References

Abdullahie Fard, I., Braathen, A., Mokhtari, M., Alavi, S.A., 2006. Interaction of the Zagros fold–thrust belt and the Arabian-type, deep-seated folds in the Abadan plain and the dezful embayment, SW Iran. Petrol. Geosci. 12, 347–362.

Ahmadhadi, F., Lacombe, O., Daniel, J.M., 2007. Early reactivation of basement faults in Central Zagros (SW Iran): evidence from pre-folding fracture populations in Asmari Formation and lower Tertiary paleogeography. In: Thrust Belts and Foreland Basins. Springer, Berlin, Heidelberg, pp. 205–228.

Al-Hajeri, M.M., Bowden, S.A., 2017. Application of formation water geochemistry to assess seal integrity of the Gotnia Formation, Kuwait. Arabian J. Geosci. 10 (3), 1–10.

Al-Hajeri, M.M., Parnell, J., Bowden, S., Costanzo, A., Feely, M., 2017. Deep hydrothermal activity in hydrocarbon reservoirs, South Kuwait. Arabian J. Geosci. 10 (2), 1–13.

Al-Husseini, M.I., 2000. Origin of the Arabian plate structures: Amar collision and Najd rift. GeoArabia 5, 527–542.

Alavi, M., 1994. Tectonics of the Zagros orogenic belt of Iran: new data and interpretations. Tectonophysics 229, 211–238.

Alavi, M., 2004. Regional stratigraphy of the Zagros fold-thrust belt of Iran and its proforeland evolution. Am. J. Sci. 304, 1–20.

Alavi, M., 2007. Structures of the Zagros fold-thrust belt in Iran. Am. J. Sci. 307, 1064–1095.

Asgari, G., Ghaemi, F., Soleimany, B., Rahimi, B., Shekarian, Y., 2019. Role of incompetent strata and geometry of faults on the folding mechanism, a case study: the Karun oilfield in the Dezful Embayment, Iran. Model. Earth Syst. Environ. 5 (4), 1781–1800.

Asl, M.E., Faghih, A., Mukherjee, S., Soleimany, B., 2019. Style and timing of salt movement in the Persian Gulf basin, offshore Iran: insights from halokinetic sequences adjacent to the Tonb-e-Bozorg salt diapir. J. Struct. Geol. 122, 116–132.
Bahroudi, A., Koyi, H.A., 2003. Effect of spatial distribution of Hormuz salt on deformation style in the Zagros fold-and-thrust belt: an analogue modelling approach. J. Geol. Soc. 160, 719–733.
Bahroudi, A., Talbot, C.J., 2003. The configuration of the basement beneath the Zagros Basin. J. Petrol. Geol. 26, 257–282.
Baniasad, A., Sachse, V., Littke, R., Soleimany, B., 2019. Burial, temperature and maturation history of cretaceous source rocks in the NW Persian Gulf, offshore SW Iran: 3D basin modelling. J. Petrol. Geol. 42 (2), 125–144.
Baniasad, A., Littke, R., Froidl, F., Grohmann, S., Soleimany, B., 2021. Quantitative hydrocarbon generation and charge risk assessment in the NW Persian Gulf: a 3D basin modeling approach. Mar. Petrol. Geol. 126, 104900.
Barrier, L., Nalpas, T., Gapais, D., Proust, J.N., Casas, A., Bourquin, S., 2002. Influence of syntectonic sedimentation on thrust geometry. Field examples from the Iberian Chain (Spain) and analogue modelling. Sediment. Geol. 146 (1–2), 91–104.
Beauchamp, W., Campbell, D.S., Ventures, A.M.E.N., Guilford, U.K., Roshandel, H., Motiei, H., 2000. Structural styles of the dezful embayment, Zagros Mountains, Iran. In: 2000 AAPG Annual Meeting.
Berberian, M., 1995. Master "blind" thrust faults hidden under the Zagros folds: active basement tectonics and surface tectonics surface morphotectonics. Tectonophysics 241, 193–224.
Berberian, M., King, G.C.P., 1981. Towards a paleogeography and tectonic evolution of Iran. Can. J. Earth Sci. 18, 210–265.
Beydoun, Z.R., 1991. Arabian plate hydrocarbon geology and potential. In: A Plate Tectonic Approach. American Association of Petroleum Geologists, pp. 1–77.
Bordenave, M.L., Hegre, J.A., 2005. The influence of tectonics on the entrapment of oil in the Dezful Embayment, Zagros Fold belt, Iran. J. Petrol. Geol. 28 (4), 339–368.
Buchanan, J.G., Buchanan, P.G., 1995. In: Basin Inversion, vol. 88. Geological Society of London, p. 606. Special Publication.
Bulnes, M., Poblet, J., 1999. Estimating the detachment depth in cross-sections involving detachment folds. Geol. Mag. 136 (4), 395–412.
Burberry, C.M., Swiatlowski, J.L., 2016. Evolution of a fold-thrust belt deforming a unit with pre-existing linear asperities: insights from analog models. J. Struct. Geol. 87, 1–18.
Butler, R.W., Tavarnelli, E., Grasso, M., 2006. Structural inheritance in mountain belts: an Alpine–Apennine perspective. Journal of Structural Geology 28 (11), 1893–1908.
Carruba, S., Perotti, C.R., Buonaguro, R., Calabrò, R., Carpi, R., Naini, M., 2006. The structural pattern of the Zagros fold-and-thrust belt in the Dezful Embayment (SW Iran). Spec. Pap. Geol. Soc. Am. 414, 11.
Casciello, E., Vergés, J., Saura, E., Casini, G., Fernandez, N., Blanc, E., Homke, S., Hunt, D.W., 2009. Fold patterns and multilayer rheology of the Lurestan Province, Zagros simply folded belt (Iran). J. Geol. Soc. Lond. 166, 947–959.
Castelltort, S., Pochat, S., Van Den Driessche, J., 2004. Using T-Z plots as a graphical method to infer lithological variations from growth strata. J. Struct. Geol. 26 (8), 1425–1432.
Chamberlin, R.T., 1910. The Appalachian folds of central Pennsylvania. J. Geol. 18 (3), 228–251.
Colman-Sadd, S.P., 1978. Fold development in Zagros simply folded belt, Southwest Iran. AAPG Bull. 62, 984–1003.
Cooper, M.A., Williams, G.D., 1989. Inversion structures–recognition and characteristics. In: Inversion Tectonics, vol. 44, pp. 341–347. Geological Society of London.
Cooper, M.A., Williams, G.D., De Graciansky, P.C., Murphy, R.W., Needham, T., De Paor, D., et al., 1989. Inversion tectonics—a discussion. Geol. Soc. Lond. Spec. Publ. 44 (1), 335–347.
Currie, J.B., Patnode, H.W., Trump, R.P., 1962. Development of folds in sedimentary strata. Geol. Soc. Am. Bull. 73 (6), 655–673.
Dahlstrom, C.D.A., 1990. Geometric constraints derived from the law of conservation of volume and applied to evolutionary models of detachment folding. Am. Assoc. Petrol. Geol. Bull. 74, 336–344.
Dasgupta, S., Mukherjee, S., 2017. Brittle shear tectonics in a narrow continental rift: asymmetric nonvolcanic Barmer Basin (Rajasthan, India). J. Geol. 125 (5), 561–591.
Dasgupta, T., Mukherjee, S., 2020. Sediment Compaction and Applications in Petroleum Geoscience. Springer International Publishing.
Del Ventisette, C., Montanari, D., Sani, F., Bonini, M., 2006. Basin inversion and fault reactivation in laboratory experiments. J. Struct. Geol. 28 (11), 2067–2083.
Deng, H., McClay, K., Bilal, A., 2021. Multiphase activation of the boundary fault system of the eastern Dampier sub-basin, Northwest Shelf of Australia. AAPG Bull. 105 (1), 157–188.
Derikvand, B., Alavi, S.A., Abdullahie Fard, I., Hajialibeigi, H., 2018. Folding style of the Dezful Embayment of Zagros Belt: signatures of detachment horizons, deep-rooted faulting, and syn-deformation deposition. Mar. Petrol. Geol. 91, 501–518.
DiBiase, R.A., Rossi, M.W., Neely, A.B., 2018. Fracture density and grain size control on the relief structure of bedrock landscapes. Geology 46 (5), 399–402.
Duffy, O.B., Dooley, T.P., Hudec, M.R., Jackson, M.P., Fernandez, N., Jackson, C.A., Soto, J.I., 2018. Structural evolution of salt-influenced fold-and-thrust belts: a synthesis and new insights from basins containing isolated salt diapirs. J. Struct. Geol. 114, 206–221.
Edgell, H.S., 1992. Basement tectonics of Saudi Arabia as related to oilfield structures. In: Basement Tectonics. Springer, Dordrecht, pp. 169–193.
Edgell, H.S., 1996. Salt Tectonism in the Persian Gulf Basin, vol. 100. Geological Society, London, Special Publications, pp. 129–151.
Epard, J.L., Groshong Jr., R.H., 1993. Excess area and depth to detachment. AAPG Bull. 77 (8), 1291–1302.
Falcon, N.L., 1974. Southern Iran: Zagros Mountains, vol. 4. Geological Society, London, Special Publications, pp. 199–211.
Fang, J., Zhou, F., Tang, Z., 2017. Discrete fracture network modelling in a naturally fractured carbonate reservoir in the Jingbei oilfield, China. Energies 10 (2), 183.
Faqira, M., Rademakers, M., Afifi, A.M., 2009. New insights into the Hercynian orogeny, and their implications for the Paleozoic hydrocarbon system in the Arabian plate. GeoArabia 14, 199–228.
Farahzadi, E., Alavi, S.A., Sherkati, S., Ghassemi, M.R., 2019. Variation of subsidence in the Dezful Embayment, SW Iran: influence of reactivated basement structures. Arabian J. Geosci. 12, 616.
Farzipour-Saein, A., Koyi, H., 2016. Intermediate decollement activation in response to the basal friction variation and its effect on folding style in the Zagros fold-thrust belt, an analogue modelling approach. Tectonophysics 68, 56–65.
Farzipour-Saein, A., Nilfouroushan, F., Koyi, H., 2013. The effect of basement step/topography on the geometry of the Zagros fold-and-thrust belt (SW Iran): an analog modelling approach. Int. J. Earth Sci. 102, 2117–2135.
Giambiagi, L.B., Alvarez, P.P., Godoy, E., Ramos, V.A., 2003. The control of pre-existing extensional structures on the evolution of the southern sector of the Aconcagua fold and thrust belt, southern Andes. Tectonophysics 369 (1–2), 1–19.
Giambiagi, L., Ghiglione, M., Cristallini, E., Bottesi, G., 2009. Kinematic models of basement/cover interaction: insights from the Malargüe fold and thrust belt, Mendoza, Argentina. J. Struct. Geol. 31 (12), 1443–1457.
Griffiths, P., Jones, S., Salter, N., Schaefer, F., Osfield, R., Reiser, H., 2002. A new technique for 3-D flexural-slip restoration. J. Struct. Geol. 24 (4), 773–782.
Heydarzadeh, K., Ruh, J.B., Vergés, J., Hajialibeigi, H., Gharabeigli, G., 2020. Evolution of a structural basin: numerical modelling applied to the Dehdasht basin, central Zagros, Iran. J. Asian Earth Sci. 187, 104088.
Holdsworth, R.E., Butler, C.A., Roberts, A.M., 1997. The recognition of reactivation during continental deformation. J. Geol. Soc. 154 (1), 73–78.
Husseini, M.I., 1988. The Arabian infracambrian extensional system. Tectonophysics 148, 93–103.
Husseini, M.I., 1989. Tectonic and deposition model of late Precambrian-Cambrian Arabian and adjoining plates. AAPG Bull. 73, 1117–1131.
Jahani, S., Hassanpour, J., Mohammadi-Firouz, S., Letouzey, J., de Lamotte, D.F., Alavi, S.A., Soleimany, B., 2017. Salt tectonics and tear faulting in the central part of the Zagros Fold-Thrust Belt, Iran. Mar. Petrol. Geol. 86, 426–446.
Konert, G., Afifi, A.M., Al-Hajri, S.A., de Groot, K., Al Naim, A.A., Droste, H.J., 1999. Paleozoic stratigraphy and hydrocarbon habitat of the Arabian plate. AAPG Bull. 83, 1320–1336.
Koop, W.J., Stoneley, R., 1982. Subsidence history of the Middle East Zagros basin, Permian to recent. Phil. Trans. Roy. Soc. Lond. A Math. Phys. Sci. 305 (1489), 149–168.
Kosari, E., Kadkhodaie, A., Bahroudi, A., Chehrazi, A., Talebian, M., 2017. An integrated approach to study the impact of fractures distribution on the Ilam-Sarvak carbonate reservoirs: a case study from the Strait of Hormuz, the Persian Gulf. J. Petrol. Sci. Eng. 152, 104–115.
Koukouvelas, I.K., Zygouri, V., Papadopoulos, G.A., Verroios, S., 2017. Holocene record of slip-predictable earthquakes on the Kenchreai fault, Gulf of Corinth, Greece. J. Struct. Geol. 94, 258–274.
Koyi, H., Nilfouroushan, F., Hessami, K., 2016. Modelling role of basement block rotation and strike-slip faulting on structural pattern in cover units of fold-and-thrust belts. Geol. Mag. 153 (5–6), 827–844.
Letouzey, J., Werner, P., Marty, A., 1990. Fault reactivation and structural inversion. Backarc and intraplate compressive deformations. Example of the eastern Sunda shelf (Indonesia). Tectonophysics 183 (1–4), 341–362.
Marshak, S., Wilkerson, M.S., 1992. Effect of overburden thickness on thrust belt geometry and development. Tectonics 11 (3), 560–566.
McClymont, A.F., Villamor, P., Green, A.G., 2009. Fault displacement accumulation and slip rate variability within the Taupo Rift (New Zealand) based on trench and 3-D ground-penetrating radar data. Tectonics 28 (4).
McQuillan, H., 1991. The role of basement tectonics in the control of sedimentary facies, structural patterns, and salt plug emplacements in the Zagros fold belt of southwest Iran. J. Southeast Asian Earth Sci. 5, 453–463.
Meng, Q., Hodgetts, D., 2019. Combined control of décollement layer thickness and cover rock cohesion on structural styles and evolution of fold belts: a discrete element modelling study. Tectonophysics 757, 58–67.
Misra, A.A., Mukherjee, S., 2015. Tectonic Inheritance in Continental Rifts and Passive Margins. Springer briefs in Earth Sciences, ISBN 978-3-319-20576-2.
Mitra, S., 2002. Structural models of faulted detachment folds. AAPG Bull. 86 (9), 1673–1694.
Moghadam, H.S., Stern, R.J., Chiaradia, M., Rahgoshay, M., 2013. Geochemistry and tectonic evolution of the late cretaceous Gogher–Baftophiolite, central Iran. Lithos 168, 33–47.
Motamedi, H., Sherkati, S., Sepehr, M., 2012. Structural style variation and its impact on hydrocarbon traps in central Fars, southern Zagros folded belt, Iran. J. Struct. Geol. 37, 124–133.
Motiei, H., 1994. Stratigraphy of Zagros. Report (In Farsi). Geol Surv of Iran, Tehran.
Motiei, H., 1995. Petroleum Geology of Zagros (In Farsi). Geol Surv of Iran, Tehran.
Mouthereau, F., Tensi, J., Bellahsen, N., Lacombe, O., De Boisgrollier, T., Kargar, S., 2007. Tertiary sequence of deformation in a thin-skinned/thick-skinned collision belt: the Zagros Folded Belt (Fars, Iran). Tectonics 26 (5).
Mouthereau, F., Lacombe, O., Vergés, J., 2012. Building the Zagros collisional orogen: timing, strain distribution and the dynamics of Arabia/Eurasia plate convergence. Tectonophysics 532, 27–60.

Mukherjee, S., 2011. Estimating the viscosity of rock bodies: a comparison between the Hormuz-and the Namakdan salt domes in the Persian Gulf, and the Tso Morari gneiss dome in the Himalaya. Indian J. Geophys. Union 15 (3), 161–170.
Mukherjee, S., Talbot, C.J., Koyi, H.A., 2010. Viscosity estimates of salt in the Hormuz and Namakdan salt diapirs, Persian Gulf. Geol. Mag. 147 (4), 497–507.
Nabavi, S.T., Fossen, H., 2021. Fold geometry and folding–a review. Earth Sci. Rev. 222, 103812.
Najafi, M., Yassaghi, A., Bahroudi, A., Vergés, J., Sherkati, S., 2014. Impact of the late Triassic Dashtak intermediate detachment horizon on anticline geometry in the central frontal Fars, SE Zagros fold belt, Iran. Mar. Petrol. Geol. 54, 23–36.
Najafi, M., Vergés, J., Etemad-Saeed, N., Karimnejad, H.R., 2018. Folding, thrusting and diapirism: competing mechanisms for shaping the structure of the north Dezful Embayment, Zagros, Iran. Basin Res. 30 (6), 1200–1229.
Narr, W., Currie, J.B., 1982. Origin of fracture porosity—example from Altamont field, Utah. AAPG Bull. 66 (9), 1231–1247.
Noori, H., Mehrabi, H., Rahimpour-Bonab, H., Faghih, A., 2019. Tectono-sedimentary controls on Lower Cretaceous carbonate platforms of the central Zagros, Iran: an example of rift-basin carbonate systems. Mar. Petrol. Geol. 110, 91–111.
Orang, K., Gharabeigli, G., 2020. Tectonostratigraphic evolution of the Helleh paleo-high (NW Persian Gulf): insights from 2D and 3D restoration methods. Mar. Petrol. Geol. 119, 104443.
Pash, R.R., Sarkarinejad, K., Ghoochaninejad, H.Z., Motamedi, H., Yazdani, M., 2020. Accommodation of the different structural styles in the foreland fold-and-thrust belts: northern Dezful Embayment in the Zagros belt, Iran. Int. J. Earth Sci. 109 (3), 959–970.
Perotti, C.R., Carruba, S., Rinaldi, M., Bertozzi, G., Feltre, L., Rahimi, M., 2011. The Qatar–South Fars arch development (Arabian Platform, Persian Gulf): insights from seismic interpretation and analogue modelling. New Front. Tect. Res. Midst Plate Convergence 13, 325–352.
Pichot, T., Nalpas, T., 2009. Influence of synkinematic sedimentation in a thrust system with two decollement levels; analogue modelling. Tectonophysics 473 (3–4), 466–475.
Pirouz, M., Avouac, J.P., Hassanzadeh, J., Kirschvink, J.L., Bahroudi, A., 2017. Early Neogene foreland of the Zagros, implications for the initial closure of the Neo-Tethys and kinematics of crustal shortening. Earth Planet Sci. Lett. 477, 168–182.
Pla, O., Roca, E., Xie, H., Izquierdo-Llavall, E., Muñoz, J.A., Rowan, M.G., et al., 2019. Influence of Syntectonic sedimentation and Décollement rheology on the geometry and evolution of Orogenic wedges: analog modeling of the Kuqa fold-and-Thrust Belt (NW China). Tectonics 38 (8), 2727–2755.
Ramsay, J.G., 1967. Folding and Fracturing of Rocks. McGraw Hill Book Company, New York.
Riahi, Z.T., Sarkarinejad, K., Faghih, A., Soleimany, B., Payrovian, G.R., 2021. Impact of inversion tectonics on the spatial distribution of hydrocarbon traps in the NW Persian Gulf and the southern Dezful Embayment, SW Iran. Mar. Petrol. Geol. 134, 105364.
Rowan, M.G., Ratliff, R.A., 2012. Cross-section restoration of salt-related deformation: best practices and potential pitfalls. J. Struct. Geol. 41, 24–37.
Rowan, M.G., Muñoz, J.A., Roca, E., Ferrer, O., Santolaria, P., Granado, P., Snidero, M., 2022. Linked detachment folds, thrust faults, and salt diapirs: observations and analog models. J. Struct. Geol. 155, 104509.
Santolaria, P., Ferrer, O., Rowan, M.G., Snidero, M., Carrera, N., Granado, P., et al., 2021. Influence of preexisting salt diapirs during thrust wedge evolution and secondary welding: insights from analog modeling. J. Struct. Geol. 149, 104374.
Sarkarinejad, K., Azizi, A., 2008. Slip partitioning and inclined dextral transpression along the Zagros Thrust System, Iran. J. Struct. Geol. 30, 116–136.
Sarkarinejad, K., Goftari, F., 2019. Thick-skinned and thin-skinned tectonics of the Zagros orogen, Iran: constraints from structural, microstructural and kinematics analyses. J. Asian Earth Sci. 170, 249–273.
Schori, M., Zwaan, F., Schreurs, G., Mosar, J., 2021. Pre-existing basement faults controlling deformation in the Jura Mountains fold-and-thrust belt: insights from analogue models. Tectonophysics 814, 228980.
Scisciani, V., 2009. Styles of positive inversion tectonics in the Central Apennines and in the Adriatic foreland: implications for the evolution of the Apennine chain (Italy). J. Struct. Geol. 31 (11), 1276–1294.
Sclater, J.G., Christie, P.A., 1980. Continental stretching: an explanation of the post-mid-Cretaceous subsidence of the central North Sea basin. J. Geophys. Res. Solid Earth 85 (B7), 3711–3739.
Sepehr, M., Cosgrove, J.W., 2004. Structural framework of the Zagros fold–thrust belt, Iran. Mar. Petrol. Geol. 21, 829–843.
Sepehr, M., Cosgrove, J.W., Moieni, M., 2006. The impact of cover rock rheology on the style of folding in the Zagros fold-thrust belt. Tectonophysics 427, 265–281.
Setudehnia, A., 1978. The Mesozoic sequence in south-west Iran and adjacent areas. J. Petrol. Geol. 1, 3–42.
Sherkati, S., Letouzey, J., 2004. Variation of structural style and basin evolution in the central Zagros (Izeh zone and Dezful Embayment), Iran. Mar. Petrol. Geol. 21, 535–554.
Sherkati, S., Letouzey, J., Frizon de Lamotte, D., 2006. Central Zagros fold-thrust belt (Iran): new insights from seismic data, field observation, and sandbox modelling. Tectonics 25, TC4007.
Soleimani, M., Shokri, B.J., Rafiei, M., 2017. Integrated petrophysical modeling for a strongly heterogeneous and fractured reservoir, Sarvak Formation, SW Iran. Nat. Resour. Res. 26 (1), 75–88.
Soleimany, B., Poblet, J., Bulnes, M., Sàbat, F., 2011. Fold amplification history unraveled from growth strata: the Dorood anticline, NW Persian Gulf. J. Geol. Soc. 168, 219–234.
Srivastava, D.C., Lisle, R.J., 2004. Rapid analysis of fold shape using Bézier curves. J. Struct. Geol. 26 (9), 1553–1559.
Stampfli, G.M., Borel, G.D., 2002. A plate tectonic model for the Paleozoic and Mesozoic constrained by dynamic plate boundaries and restored synthetic oceanic isochrons. Earth Planet Sci. Lett. 196, 17–33.
Stewart, S.A., 2018. Hormuz salt distribution and influence on structural style in NE Saudi Arabia. Petrol. Geosci. 24, 143–158.
Stewart, S.A., Muslem, A.S., Wibisono, G., 2018. Triassic fault reactivation in eastern Saudi Arabia: implications for shear and fluid systems on the southern margin of Neotethys. J. Geol. Soc. 175, 619–626.
Storti, F., Poblet, J., 1997. Growth stratal architectures associated to décollement folds and fault-propagation folds. Inferences on fold kinematics. Tectonophysics 282 (1–4), 353–373.
Szabo, F., Kheradpir, A., 1978. Permian and Triassic stratigraphy, Zagros basin, south-west Iran. J. Petrol. Geol. 1, 57–82.
Talbot, C.J., Alavi, M., 1996. The past of a future syntaxis across the Zagros. In: Alsop, G. L., Blundell, D.L., Davison, I. (Eds.), Salt Tectonics, 100, pp. 89–109. Geol Soc London Spec Pub.
Tari, G., Arbouille, D., Schléder, Z., Tóth, T., 2020. Inversion tectonics: a brief petroleum industry perspective. Solid Earth 11 (5), 1865–1889.
Tavakoli-Shirazi, S., Frizon de Lamotte, D., Wrobel-Daveau, J.C., Ringenbach, J.C., 2013. Pre-Permian uplift and diffuse extensional deformation in the High Zagros Belt (Iran): integration in the geodynamic evolution of the Arabian plate. Arabian J. Geosci. 6 (7), 2329–2342.
Tong, H., Koyi, H., Huang, S., Zhao, H., 2014. The effect of multiple pre-existing weaknesses on formation and evolution of faults in extended sandbox models. Tectonophysics 626, 197–212.
Valero, L., Soleimany, B., Bulnes, M., Poblet, J., 2015. Evolution of the Nourooz anticline (NW Persian Gulf) deciphered using growth strata: structural inferences to constrain hydrocarbon exploration in Persian offshore anticlines. Mar. Petrol. Geol. 66, 873–889.
Vatandoust, M., Faghih, A., Asadi, S., Azimzadeh, A.M., Soleimany, B., 2020. Hydrocarbon migration and charge history in the Karanj, Paranj and Parsi oilfields, southern dezful embayment, Zagros fold-and-thrust belt, SW Iran. J. Petrol. Geol. 43 (3), 341–357.
Vergés, J., Saura, E., Casciello, E., Fernandez, M., Villaseñor, A., Jimenez-Munt, I., García-Castellanos, D., 2011. Crustal-scale cross-sections across the NW Zagros belt: implications for the Arabian margin reconstruction. Geol. Mag. 148, 739–761.
Yaghoubi, A., 2019. Hydraulic fracturing modeling using a discrete fracture network in the Barnett Shale. Int. J. Rock Mech. Min. Sci. 119, 98–108.
Ziegler, P.A., Cloetingh, S., van Wees, J.D., 1995. Dynamics of intra-plate compressional deformation: the Alpine foreland and other examples. Tectonophysics 252 (1–4), 7–59.

Further Reading

Butler, R.W., Bond, C.E., Cooper, M.A., Watkins, H., 2018. Interpreting structural geometry in fold-thrust belts: Why style matters. Journal of Structural Geology 114, 251–273.
Cooper, M., Warren, M.J., 2020. Inverted fault systems and inversion tectonic settings. In: Scarselli, N., et al. (Eds.), Regional Geology and Tectonics (Second Edition). Elsevier, pp. 169–204.
Coward, M.P., 1994. Inversion tectonics. In: Hancock, P.L. (Ed.), Continental deformation. Pergamon Press, New York, pp. 289–304.
Karimnejad Lalami, H.R., Hajialibeigi, H., Sherkati, S., Adabi, M.H., 2020. Tectonic evolution of the Zagros foreland basin since Early Cretaceous, SW Iran: regional tectonic implications from subsidence analysis. Journal of Asian Earth Sciences 204. https://doi.org/10.1016/j.jseaes.2020.104550.
McClay, K.R., 1989. Analogue models of inversion tectonics. Geological Society, London, Special Publications 44 (1), 41–59.
Shamszadeh, A., Sarkarinejad, K., Ferrer, O., Mukherjee, S., Seraj, M., 2022. Effect of inherited structural highs on the structure and kinematics of the South Dezful Embayment, SW Iran. Geological Magazine 1–23. https://doi.org/10.1017/S0016756822000541.